University of Palermo

Department of Biological Chemical and Pharmaceutical Sciences and Technology

(**STEBICEF**)

PhD in Cell Biology

(Cell Biology and Development)

XXIV CYCLE

Regulation of physiological differentiation in *Nonomuraea* sp. *ATCC 39727*

Scientific area code **BIO 19**

PhD student **Letizia Lo Grasso**

Tutor: Prof. A. M. Puglia

Cotutor: Dott. R. Alduina

PhD coordinator: Prof. Gabriella Sconzo

Abstract

The Actinomycete *Nonomuraea* produces the glycopeptide A40926, precursor of dalbavancin, a novel lipoglycopeptide homologous to vancomycin that could be used against emerging resistant Gram-positive bacteria. The A40926 biosynthetic gene cluster (*dbv*), which consists of 37 genes, encodes two regulators, Dbv3 (LuxR-like) and Dbv4 (StrR-like), as well as the response regulator (Dbv6) and the sensor-kinase (Dbv22) of a putative two-component system. Previous work demonstrated a positive role of Dbv4 in antibiotic production by activating the transcription of 13 *dbv* genes; up to now no role was assigned to Dbv3, Dbv6 and Dbv22. In addition, an IclR-like protein is thought to be involved in *dbv4* expression. The *iclR* gene is not localized in the *dbv* cluster and encodes a putative DNA binding protein that controls growth, primary and secondary metabolism in other bacteria.

Mutants in *dbv3, dbv4, dbv6, dbv22* and *iclR* genes were independently generated, revealing that Dbv3, Dbv4 and IclR are necessary for antibiotic production, while the response regulator Dbv6 and the sensor-kinase Dbv22 do not seem to influence A40926 production.

Phenotypic analysis of the *dbv6* and *dbv22* mutants revealed that Dbv6 (VanR like) and Dbv22 (VanS like) do not influence bacterial growth, but they could control resistance; indeed, the mutants are more sensitive to vancomycin (a commercially available glycopeptide) in respect to the wild type.

Dbv3 belongs to the LAL family (Large ATP-binding regulators of the LuxR family). The LuxR transcriptional regulator is a key player of a large variety of quorum sensing

processes, regulating the expression of genes related to antibiotic biosynthesis, motility, nodulation, plasmid transfer, bioluminescence, pathogenicity, biofilm formation, etc.

Kinetic growth curves of *dbv3* mutant (Ko *dbv3*) revealed that Dbv3 does not influence bacterial growth in liquid rich medium (R3) but that it is necessary for antibiotic production. Semi-quantitative RT-PCR analysis after 48 hours of growth demonstrated that Dbv3 controls some genes involved in the antibiotic production. To further investigate the role of Dbv3 in differentiation and growth, strains that over-express *dbv3* were generated. Phenotypic analyses revealed no differences in growth on R3 medium, while antibiotic production was about two fold more abundant than in the wild type.

In experiments of affinity chromatography using as bait a DNA fragment upstream of the gene *dbv4* (called P4) a protein IclR-like was isolated, that could have a role in regulating the expression of *dbv4* gene.

IclR family comprises regulators acting as repressors, activators and proteins with a dual role (activator and repressor). Members of the IclR family control genes whose products are involved in the glyoxylate shunt, multidrug resistance, degradation of aromatics, inactivation of quorum-sensing signals, determinants of plant pathogenicity, antibiotic production and sporulation.

Since P4 is localized downstream *dbv4* transcriptional start site, mapped by S1-mapping experiments, a negative role to IclR was hypothesized. Indeed, qRT-PCR analysis showed that the levels of transcription of genes *iclR* and *dbv4* have an opposite trend: *iclR* is more transcribed when a low yield of antibiotic is produced; *dbv4,* vice versa, is more transcribed when antibiotic production is high. These preliminary data suggest a possible involvement of IclR in A40926 production.

Three knock out *iclR* mutants were generated. Morphological and physiological analysis revealed that they lost the capacity to grow on minimal medium, they were not pigmented

in the rich medium R3-agar and produced the antibiotic after 9 days of growth, while wild type produced after 3 days in the same growth condition. Different carbon sources and aminoacids were added to minimal medium to restore growth and pigmentation and to understand which metabolic pathways was under IclR control. At the same time, morphological and physiological analysis of five *iclR* over-expression mutants revealed that IclR has a negative effect on antibiotic production confirming its involvement in A40926 biosynthesis.

To investigate whether IclR directly regulates antibiotic biosynthesis, an His-tagged IclR was overproduced in *Escherichia coli* and purified. Gel mobility shift assays of different kind of DNA probe were carried out using the purified His6-tagged IclR. No bindings were detected. This could be due to an incorrect protein folding or to the need of some cofactors to help the protein to bind DNA.

This study provides new insights into gene expression in gram-positive bacteria, specifically focusing on the complex regulatory network governing both growth and secondary metabolism.

Introduction

Actinomycetes

Actinomycetes are soil-dwelling Gram-positive bacteria that have an unusually complex life cycle, which makes them particularly interesting for the study of bacterial development. Moreover, they are industrially relevant as producers of a wide range of bioactive secondary metabolites, including many antibiotics of clinical and commercial importance.

The understanding of actinomycete biology has been based on extensive studies on the model organism *Streptomyces coelicolor* over many years and on the availability of its complete genome sequence (Bentley *et al*, 2002). After spore germination, vegetative growth leads to formation of a mycelium consisting of a ramifying network of syncytial hyphae that penetrate a moist substrate by extension of hyphal tips and subapical branching. Subsequent reproductive growth often proceeds with the formation of filamentous aerial hyphae that eventually undergo differentiation into chains of unigenomic spores (Fig. 1)

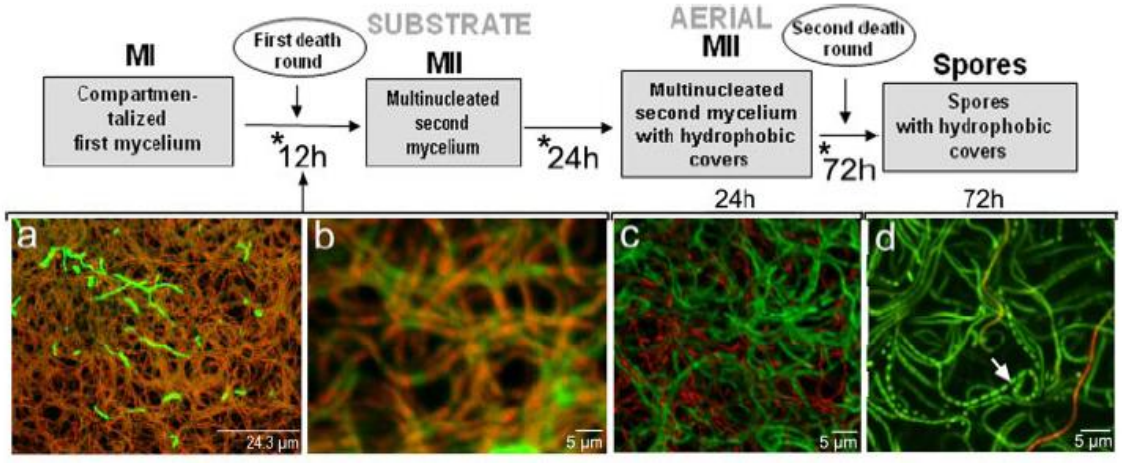

Fig. 1) Cell cycle features of *Streptomyces* development. Mycelial structures (MI, first compartmentalized mycelium; MII, second early and late multinucleated mycelia), cell death processes, and traditional denomination ("substrate" and "aerial") are indicated. Developmental time points at which samples were collected are indicated by an *asterisk*. *a–d*, confocal lasers canning fluorescence microscopy analysis of horizontal sections of cultures (Manteca *et al.* 2010).

This complex developmental cycle includes programmed cell death phenomena that make this bacterium a multicellular prokaryotic model. There are two differentiated mycelial stages: an early compartmentalized vegetative mycelium (first mycelium) and a multinucleated reproductive mycelium (second mycelium) arising after programmed cell death processes (Manteca *et al.* 2010).

Morphological differentiation in actinomycetes is strictly related to physiological differentiation: indeed the onset of morphological differentiation generally coincides with the production of secondary metabolites, such as antibiotics.

During cell death, degradative proteins are synthesized and involved in an extensive degradation of some cellular constituents (proteins and lipids) used for a second growth phase. This phenomenon accompanies antibiotic production: antibiotic could serve to protect nutrients released from dead cells or by other soil bacteria; antibiotic, naturally produced in low amounts, could act as signal molecules or hormones to coordinate the developmental cycle.

If on one hand, many factors with pleiotropic activity were identified, as key players to control both morphological and physiological differentiation in *S. coelicolor*, on the other hand for most actinomycetes mechanisms and factors governing morphological and physiological processes were not deeply investigated.

The focus of this project is the Gram positive bacterium *Nonomuraea* ATCC sp. 39727.

The kind *Nonomuraea*, before Actinomadura or also Microtetraspora (Monciardini, 2004), comprising 134 different strains, one of which is *Nonomuraea* sp. ATCC39727, an aerobic actinomycete genetically and physiologically poorly characterized.

A peculiar aspect of *Nonomuraea* sp. ATCC39727 is represented by morphological and pigmentation changes that occur during growth: on a solid rich medium (R3-Agar), *Nonomuraea* undergoes changes in morphology (it shows a “rose” shape, with notched colony side) and in pigmentation (from white to pink and purple), but it does not produce

spores (Fig. 2). Approximately after 3 days of growth, it produces the glycopeptide A40926 (Fig. 3). A40926 is similar to vancomycin, the antibiotic of last resort against multi-drug resistant pathogens. The antibiotic dalbavancin, derived by semy-synthetic process by A40926 and belonging to the teicoplanin family, is a semi synthetic lipoglycopeptide for treatment of infections by multi-resistant gram-positive bacteria, in phase III of clinical trials.

Fig. 2) Morphology of *Nonomuraea* colonies

Glycopeptides

The glycopeptides are a class of antibiotics with a complex chemical structure of very high molecular weight. Up to now about 50 glycopeptides were isolated, but only two, Vancomycin (produced by the strain *Amycolatopsis orientalis*) and Teicoplanin (produced by *Actinoplanes teichomyceticus*), are on the market and used for the treatment of persistent infections by Gram-positive multi - resistant pathogens.

Chemically, this family of glycopeptide antibiotics consists of a heptapeptide core constituted by proteinogenic and non-proteinogenic amino acids, such as 3,5-dihydroxyphenylglycine (DPG) and 4-hydroxyphenylglycine (HPG). The heptapeptides are assembled by nonribosomal peptide synthetases (NRPS) and then modified by oxidative cross-linking of the electron-rich aromatic side chains that make the peptide scaffold rigid. Further tailoring steps may include halogenation, glycosylation, methylation, acylation, and sulfation.

A40926 was originally described as a complex of related compounds differing by the type of N-acyl chain attached to the glucoronic acid moiety and for the presence or absence of an O-linked acetyl residue at position 6 of the mannose (Goldstein *et al.,* 1987; Waltho *et al.,* 1987), giving rise to compounds 1 and 2, respectively (Fig. 3). Recently, it was demonstrated that *dbv23* gene is responsible for adding the acetyl group to the mannose moiety and that compound **1** is most likely the end product of the pathway (Sosio *et al.,* 2010).

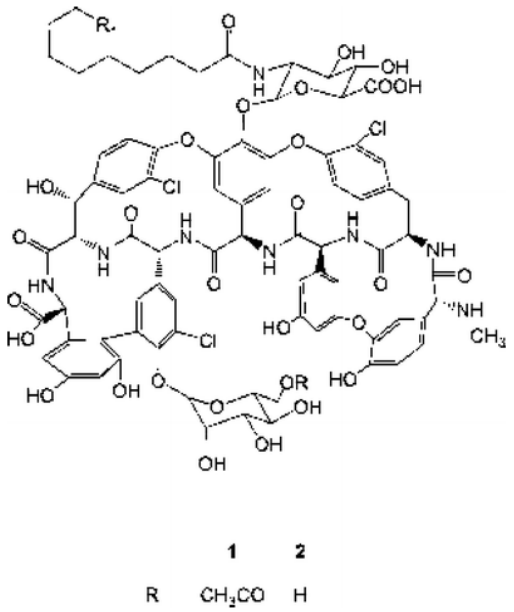

Fig.3 Structure of A40926.

The Gram-negative bacteria are naturally resistant to lycopeptides for the inability of these molecules, rather voluminous, to cross the external lipid membrane.

The bacterial cell wall of Gram-positive bacteria is characterized by a thick layer of peptidoglycan (Fig. 4): it is a crystal lattice structure formed from linear chains of two alternating amino sugars, namely *N*-acetylglucosamine (GlcNAc or NAG) and *N*-acetylmuramic acid (MurNAc or NAM). The alternating sugars are connected by a β-(1,4)-glycosidic bond. Each MurNAc is attached to a short (4- to 5-residue) amino acid chain, containing L-alanine, D-glutamine, L-lysine, and one or two D-alanine with a 5-glycine interbridge between tetrapeptides. The D- amino acids in the third position are essential for the cross-linking of the peptidoglycan chain. The peptide cross-link is formed by a transpeptidase between the free amine of the D-amino acid in the third position of a peptide chain and the D-alanine in the fourth position of another chain. The precursor form of the peptide has an extra D-alanine, which is released during the cross-linking step.

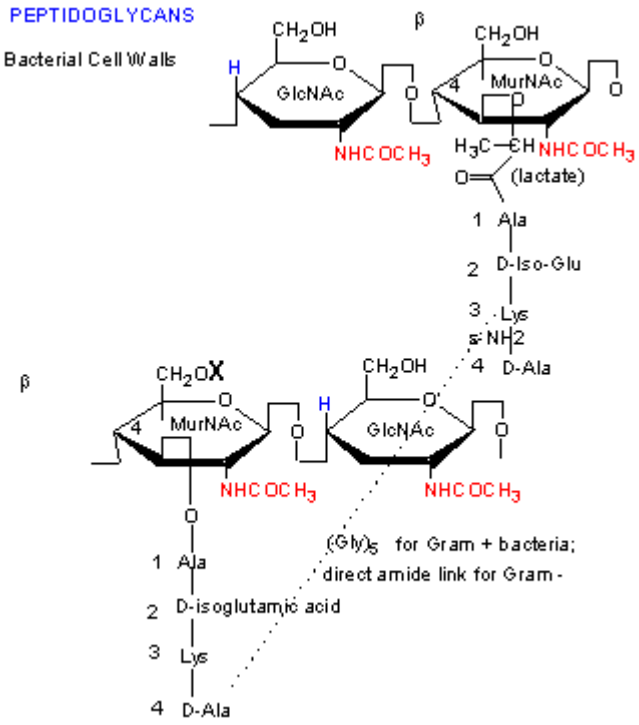

Fig 4) Chemical structure of peptidoglycan.

Glycopeptides inhibit the synthesis of cell wall in susceptible microbes by inhibiting peptidoglycan synthesis. The glycopeptides act by complexing the dimer D-Ala-D-Ala basal unit of the peptidoglycan through the formation of five hydrogen bonds. This interaction prevents transglycosylation and transpeptidation reactions, required for the insertion of the units in the basal area of growth of the peptidoglycan, resulting in cell lysis and death of the bacterium sensitive to glycopeptides.

A40926 biosynthesis

The *dbv* gene cluster for the biosynthesis of A40926 includes 37 open reading frames participating in antibiotic biosynthesis, regulation, resistance, and export (Fig. 5).

Putative roles were assigned by sequence analysis to most of the 37 *dbv* ORFs (Sosio *et al*., 2003).

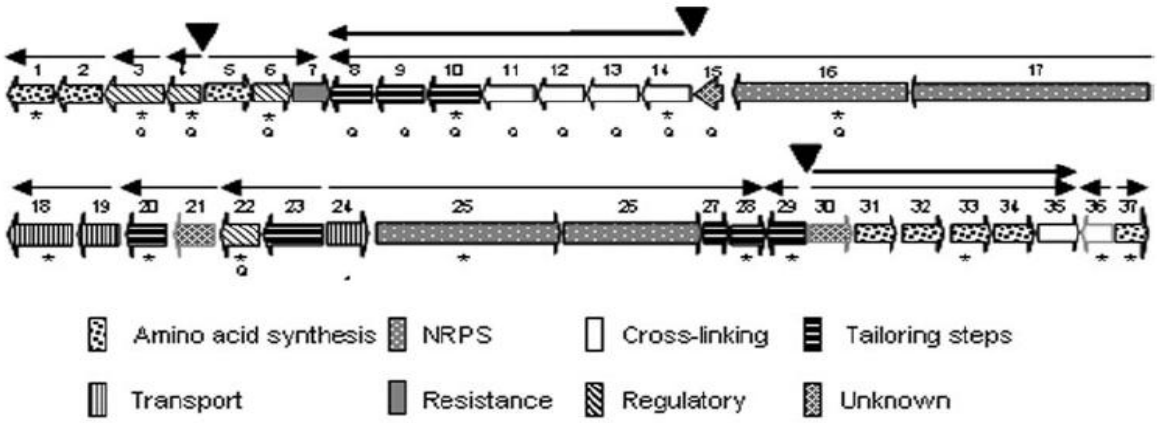

Fig 5) *dbv* cluster in *Nonomuraea*

Formation of the A40926 heptapeptide skeleton requires the specialized synthesis of three amino acids: hydroxyphenylglycine (HPG), dihydroxyphenylglycine (DPG), and β-hydroxytyrosine (βHT). *dbv1* and *dbv2* show considerable sequence identity to Hmo and *p*-hydroxymandelate synthetase (HmaS), respectively, which are required to convert *p*-hydroxyphenylpyruvate into *p*-hydroxyphenylglyoxylate during HPG synthesis in vancomycin biosynthesis (Hubbard *et al.*, 2000; Li *et al*., 2001). *dbv31* to *dbv34* are closely related to DpgA through DpgD, respectively required for DPG formation (Chen *et al.*, 2001; Pfeifer *et al.*, 2001). *dbv*37 encodes a homolog of HpgT, the amino transferase required for the transamination of both *p*-hydroxyphenylglyoxylate and 3,5-dihydroxyphenyl-glyoxylate, to yield HPG and DPG, respectively. *dbv*5, which encodes a homolog of prephenate dehydrogenase, may also participate in HPG synthesis (Hubbard *et al.*, 2000; Pfeifer *et al.*, 2001).

Synthesis of the A40926 heptapeptide precursor is catalyzed by a nonribosomal peptide synthetase (NRPS, Fig. 6).

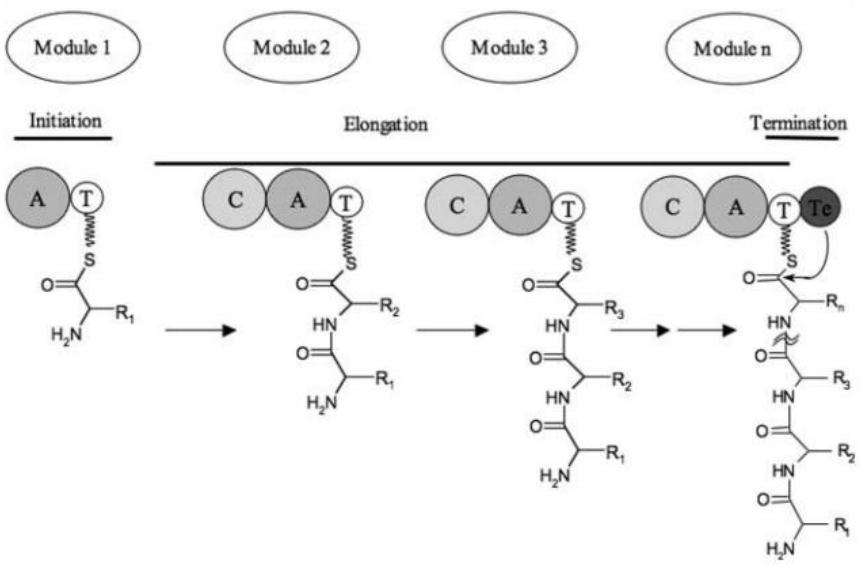

Fig. 6) General scheme of NRPS. Each NRPS module incorporates one amino acid into the growing peptide chain. The modules are composed of several domains: Adenylation domain (A) is responsible for substrate selectivity, peptidyl carrier protein domain (T) and condensation domain (C) work synergistically to form the peptide bond, and thioester domain (TE) which terminates the reaction, resulting in either a linear or cyclic polypeptide (Donadio *et al*., 2007)

In NRPSs, each elongating module is characterized by the presence of at least three domains: an adenylation domain responsible for substrate recognition and activation, a thiolation domain, which covalently binds amino acids and elongating peptides as thioesters; and a condensation domain, which catalyzes peptide bond formation. The initiation module does not usually contain a condensation domain. In addition to these core domains, an epimerization domain is usually present in those modules that convert an L amino acid into the D form. The last module is usually completed by a thioesterase domain, which hydrolyzes the thioester bond linking the completed peptide to the NRPS (Marahiel, 1997). The *dbv*16, *dbv*17, *dbv*25, and *dbv*26 encode the 7-module NRPS required for A40926 formation. *dbv*15 encodes a short, highly conserved peptide of unknown function, specified by many actinomycete clusters containing NRPS genes.

*dbv*36 encodes a type II thioesterase that could hydrolyze misprimed or misacylated thiolation domains.

The A40926 aryl groups are joined by three ether links and one C-C link carried out by P450 monooxygenases encoded by three separate *oxy* genes. *dbv*11, 12, and 14, which are best related to OxyC, OxyB, and OxyA, respectively, are involved in cross-linking of amino acids 5–7, 4–6, and 2–4. By exclusion, *dbv*13 should be involved in cross-linking of amino acids 1–3.

One chlorine atom is present on one residue each of βHT and DPG in A40926. A single halogenase gene, specified by *dbv*10, is present in the *dbv* cluster (Bischoff *et al.,* 2001). Interestingly, the presence of chlorine atoms appears to enhance antibacterial activity in some glycopeptides (Nagarajan, 1993). The following modifications are expected to occur on the newly formed A40926 aglycone: *N*-methylation of the terminal HPG residue, addition of a glucosamine moiety to the hydroxyl group of amino acid 4, *N*-acylation of the glucosamine residue, oxidation of the primary alcohol of the glucosamine moiety to yield a carboxyl group, and addition of a mannose residue to the hydroxyl group of amino acid 7. Five proteins, encoded by *dbv*9, 20, 23, 27, and 29, are likely to be involved in these tailoring steps. *dbv*9 is a glycosyltransferase, which glycosylates amino acid 4 (Solenberg *et al.,* 1997; Losey *et al.,* 2001). *dbv*27 is likely to catalyze *N*-methylation of the terminal HPG residue (O'Brien *et al.,* 2000). *dbv*23 encodes a protein highly related to members of the acyltransferase 3 family, so it might participate in *N*-acylation. *dbv*20 is responsible of A40926 mannosylation. *dbv*29 contains motifs typical of FAD binding and shows considerable matches to other proteins described as hexose oxidases. This gene is likely to govern oxidation of the glucosamine moiety to yield the corresponding acid. In addition, the presence of a putative signal sequence at the N terminus suggests that the product of *dbv*29 is secreted, and hence that oxidation occurs outside the cytoplasm.

*dbv*7 contains motifs typical of the VanY-family of carboxypeptidases, that are enzymes involved in the extracytoplasmic removal of the terminal alanine residue from nascent peptidoglycan, reducing the extent of glycopeptide binding to its molecular target. *dbv*7, thus, is involved in conferring some level of A40926 resistance to the producing strain (Binda *et al.*, 2012; Binda *et al.*,2013).

Four *dbv* genes are likely to encode export functions: *dbv*24, *dbv*35, *dbv*18 and *dbv*19.

Finally, the cluster encodes the regulators Dbv3 (LuxR-like) and Dbv4 (StrR-like), as well as the response regulator Dbv6 and the sensor-kinase Dbv22, that may be part of a two-component system.

Dalbavancin is synthesized from A-40926 in a three-step procedure. An important step in the synthesis of dalbavancin is the amidation of the peptide carboxyl group, resulting in improved potency of dalbavancin against staphylococci. The removal of the acetylglucosamine group was an intentional effort to improve the activity of dalbavancin. Additionally, dalbavancin has an acylaminoglucuronate instead of an acylglucosamine on ring. The long lipophilic side chain serves a dual purpose by both extending the halflife, which allows for once-weekly dosing, as well as anchoring the compound to the membrane, which enhances its antimicrobial activity by improving its affinity for the terminal D-Ala-D-Ala.

Regulation and Regulators of A40926 production

- **Stringent response**

In several microorganisms, such as *Nocardia* species (Ishikawa *et al.*, 2006), the production of antibiotics and other secondary metabolites occurs following the restriction of specific nutrients, such as nitrogen compounds and phosphate. The lack of specific nutrients is perceived by microorganisms through complex signaling mechanisms (Fig. 7). The study of these pathways is often the key to the understanding of regulatory processes underlying the synthesis of secondary metabolites.

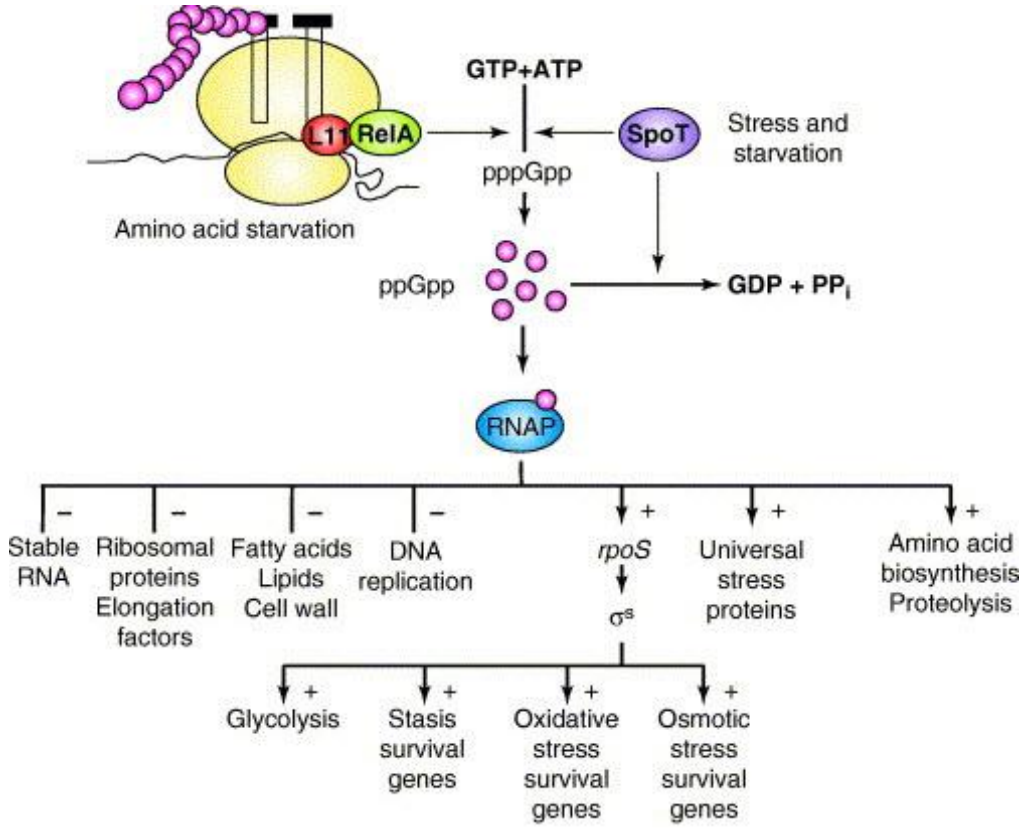

Fig. 7) Diagram of the bacterial stringent response system. Two parallel pathways synthesize pppGpp (which is subsequently converted into ppGpp) from ATP and GTP in response to any of several stress signals. Through interactions with RNA polymerase (RNAP), ppGpp alters much of metabolism. - indicates inhibition; + indicates stimulation (Magnusson *et al*, 2005)

In some bacteria of the phylum Actinobacteria, such as *Streptomyces lividans* and *Streptomyces coelicolor*, a shortage of nitrogen compounds is reflected in the increased concentration of tRNA discharges, a consequence of the limited availability of amino acids; this phenomenon leads to the activation of Rel A protein that binds ribosome stalling and allows the synthesis of the nucleotide ppGpp (guanine 5'- diphosphate 3'- diphosphate , or GDP- 3'difosphate). In conditions of nutrient deficiency, the ppGpp is accumulated and binds to the RNA polymerase subunit (encoded by the *rpoB* gene), directing the transcription of genes important for the production of secondary metabolites. This mechanism of adaptation to changes in environmental conditions is called "stringent response" (Donadio *et al*., 2008; Talà *et al*., 2009).

- **Merodiploidy of *rpoB* in *Nonomuraea***

Several actinomycetes possess two *rpoB* genes (e.i. *Nocardia species*), in contrast to the widely accepted consensus of the existence of a single RNA Polimerase (RNAP) in bacteria. In *Nonomuraea* sp. strain ATCC 39727**,** $rpoB^{(S)}$ and $rpoB^{(R)}$ provide the microorganism with two functionally distinct and developmentally regulated RNAPs (Vigliotta *et al*., 2004; Talà *et al*., 2009). $rpoB^{(R)}$ is characterized by an 18-bp in-frame deletion and mutations causing five amino acid substitutions (H426N, S431N, F445M, S474Y, and M581D), located within or close to the so-called *rif* cluster that play a key role in fundamental activities of RNAP. $rpoB^{(R)}$ transcription is tightly regulated during *Nonomuraea* growth. Indeed, transcriptional analysis demonstrated that expression of the $rpoB^{R}$ allele is growth phase-dependent in the wild type strain: the allele was silent during the pseudo-exponential phase of growth and began to be expressed during the transition to the stationary phase. Moreover, the constitutive expression of $rpoB^{(R)}$ gene increased the production of the glycopeptide antibiotic A40926 in this organism.

The merodiploidy might contribute to the developmental strategy of this actinomycete. *rpoB*$^{(R)}$ and *rpoB*$^{(S)}$ gene products may contribute to assemble growth phase-specific variants of RNA polymerase with different functional properties

- **RNA decay**

Polynucleotide phosphorylase (PNPase) has been extensively studied in *Streptomyces*. It catalyses the 3′–5′ phosphorolysis of RNAs and can also produce ribopolymers, using nucleoside diphosphates as substrates. Because of this latter activity, PNPase provides RNAs with 3′-tails that contain significant levels of G, C and U in addition to A residues that facilitate RNA degradation (Bralley and Jones, 2002). In contrast, in other bacteria including *Escherichia coli*, the major enzyme responsible for 3′-tailing of RNA is a poly(A) polymerase (Cao and Sarkar, 1992), an enzyme that is absent in streptomycetes. In these latter bacteria PNPase might be the unique RNA 3′-polynucleotide polymerase (Bralley and Jones, 2003). Evidence is provided that ppGpp acts as a negative modulator of the *Nonomuraea sp*. PNPase activity during the transition into the stationary phase thereby representing a novel link between (p)ppGpp, secondary metabolism and mRNA turnover. So (p)ppGpp may exert a modulatory effect on gene expression at the level of RNA decay also. In *E. coli*, a fast-growing microorganism with a poor secondary metabolism arsenal, ATP slows down phosphorolytic mRNA decay at high-energy charge (Del Favero *et al*., 2008) while ppGpp accelerates PNPase activity, presumably during the stationary phase. In *Nonomuraea*, a slow-growing microorganism with a rich arsenal of secondary metabolites, ppGpp slows down mRNA decay during the stationary phase, when production of secondary metabolites maximally occurs. Thus, different regulatory patterns may reflect different life styles (Siculella *et al*., 2010).

- **Phosphate control**

Apart from carbon, nitrogen and oxygen, phosphorus is the most important nutrient for living cells and since the concentration of free phosphate is usually low in natural environments, such as soil and water, free-living bacteria have developed physiological mechanisms for coping with phosphate starvation. In *Streptomyces coelicolor* phosphate controls antibiotic biosynthesis by the two-component PhoR-PhoP system (Fig. 8). The PhoR protein is a membrane sensor kinase, whereas PhoP is a member of the DNA-binding response regulators (OmpR family). PhoP activates transcription of AfsS that positively regulates secondary metabolism biosynthesis through the transcription of pathway-specific activators, like *actII-ORF4* and *redD* for actinorodin and undecilprodigiosin biosynthesis, respectively (Martín, 2004).

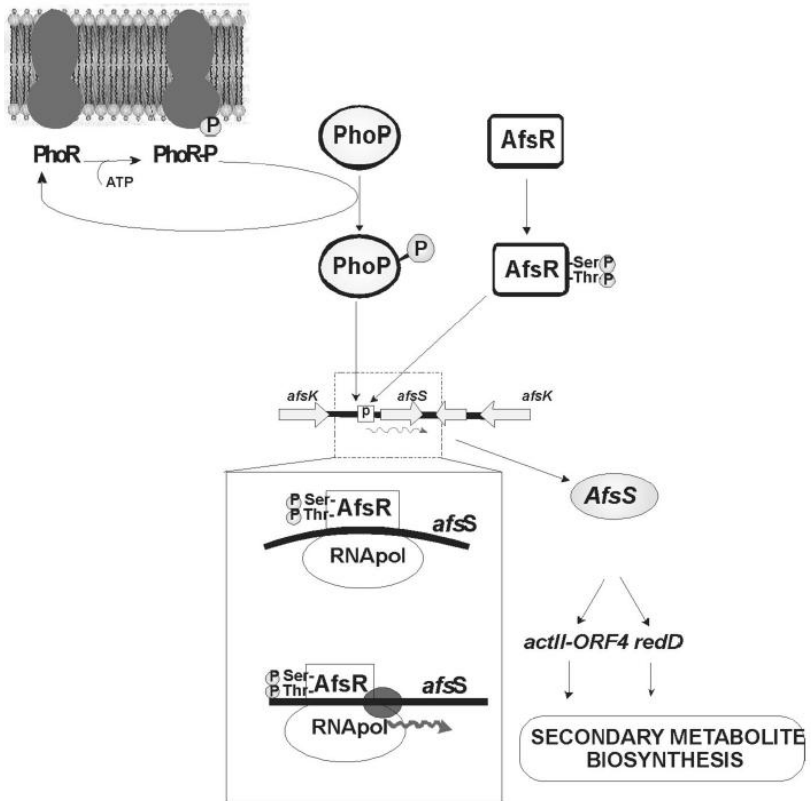

Fig.8) Proposed cascade mechanism involved in phosphate control of actinorodin and undecilprodigiosin biosynthesis in *S. coelicolor* (Martin, 2004)

Also in *Nonomuraea* A40926 production is negatively influenced by phosphate (Fig. 9). A40926 production started after 35 hours of growth in two defined media with initial phosphate concentrations of 2 mM and 4.2 mM. After 47 hours the A40964 yield was different in the two phosphate conditions: A40926 was produced in higher amount in LowP condition in respect to HighP condition. In particular, phosphate depletion induced *dbv4* transcription.

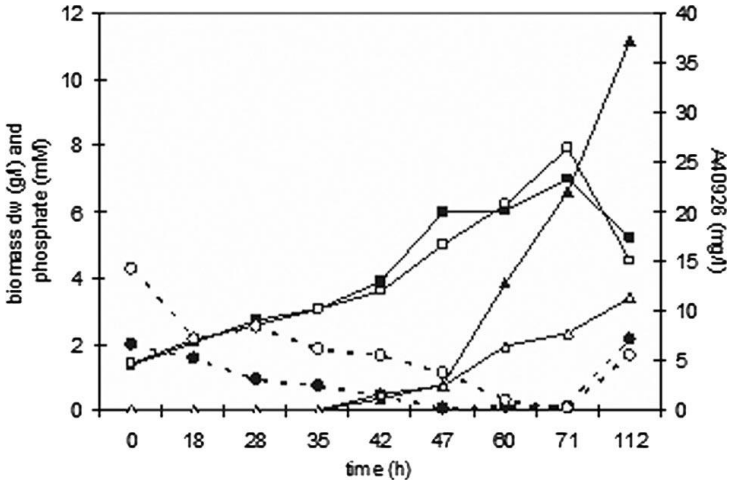

Fig.9) A40926 production in batch fermentation in *Nonomuraea*. Growth (squares), phosphate concentration (circles), and A40926 production (triangles) were monitored with initial phosphate concentrations of 2 mM (LowP; closed symbols) and 4.2 mM (HighP; open symbols) Alduina *et al*, 2007.

- **Glucose metabolism**

Actinomycete bacteria generally metabolize glucose via the Embden–Meyerhof–Parnas (EMP) and pentose-phosphate (PP) pathways (Bai *et al.*, 1975; Salas *et al.*, 1984; Dekleva and Strohl, 1988; Marx et al., 1996; Obanye et al., 1996). *Nonomuraea* metabolizes glucose mainly through the Entner–Doudoroff (ED) pathway (Fig.10), while the EMP and PP pathways are less active.

The ED pathway was discovered in *Pseudomonas saccharophila* in 1952 (Entner and Doudoroff, 1952) and was originally considered to be utilized only by a limited number of

Gram negative bacteria. However, the pathway has since been identified in a wide range of organisms within the archaea, bacteria, and eukarya (reviewed in Conway, 1992) and is evidently widespread in nature. The Entner–Doudoroff pathway also has a net yield of 1 ATP for every glucose molecule processed, as well as 1 NADH and 1 NADPH. By comparison, glycolysis has a net yield of 2 ATP and 2 NADH for each processed glucose. The ED pathway is thought to evolutionarily predate the more energetically favorable Embden–Meyerhof–Parnas (EMP) pathway (Mele´ndez – Hevia, *et al*., 1997; Romano and Conway, 1996). In some organisms, e.g., *Zymomonas mobilis* and most *Pseudomonas* species, the ED pathway is the only means of metabolizing glucose. In other cases the pathway plays a peripheral role in the central carbon metabolism, e.g., in *Escherichia coli*, where it is used for metabolism of gluconate and is induced only in the presence of this carbon source. In the actinomycete *Mycobacterium smegmatis* the contribution of the ED pathway was marginal in relation to the activities of the EMP and PP pathways (Bai *et al.*, 1976).

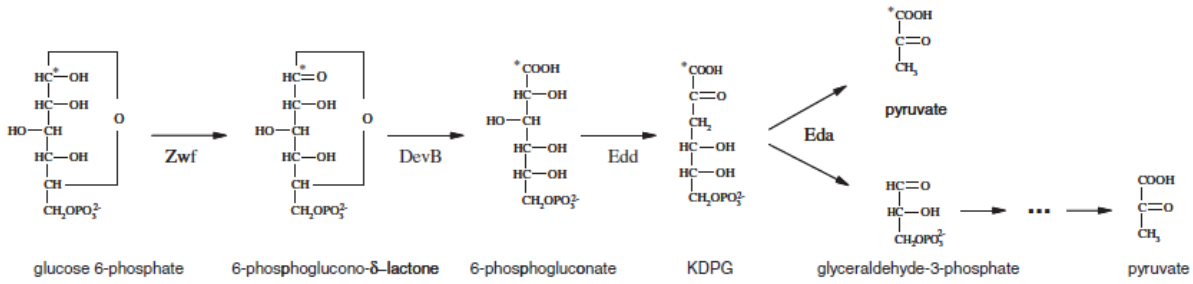

Fig. 10) Entner–Doudoroff (ED) pathway. Zwf, glucose-6-phosphate dehydrogenase; DevB, 6-phosphogluconolactonase; Edd, 6-phosphogluconate dehydratase; Eda, 2-*keto*-3-deoxy-6-phosphogluconate aldolase; KDPG, 2-*keto*-3-deoxy-6-phosphogluconate

In *Nonomuraea* a marked metabolic shift through the EMP pathway at the expense of the flux through the ED pathway was observed, shortly after phosphate depletion and in connection with the increase in A40926 antibiotic productivity.

It is therefore likely that regulation of the EMP and ED pathway activities takes place on the level of the enzymes, e.g., by phosphate inhibition or by the supply of PPi for the phosphofructokinase.

- **Cis acting regions and regulatory genes**

Sequence information is also available for five other gene clusters devoted to glycopeptides, namely, chloroeremomycin (*cep*), balhimycin (*bal*), complestatin (*com*), A47934 (*sta*), and teicoplanin (*tcp*) (Donadio *et al.*, 2005).

Four conserved stretches of non-coding DNA were identified and, interestingly, three of them are associated with segments of conserved synteny.

A 115-bp segment immediately preceding the *dpgA* start codon shows significant conservation in all five clusters (indicated as the yellow dot "a" in Fig.11). The five clusters also present a conserved 80-bp segment immediately preceding the start codon of the gene encoding the ABC transporter (indicated as the green dot "b" in Fig.11). Upstream of oxyA, a 111-bp segment is conserved in all five clusters (indicated as the light blue dot "c" in Fig.11). A highly conserved 64-nt segment is present in all clusters except *dbv* (indicated as the orange dot "d" in Fig .11).

Some of these conserved intergenic regions may represent binding sites for transcriptional regulators (e.g. the StrR-like regulator encoded in all clusters). Others might have been involved in the mobilization of gene cassettes. In any case, their existence in otherwise divergent clusters suggests important role(s) for these conserved elements.

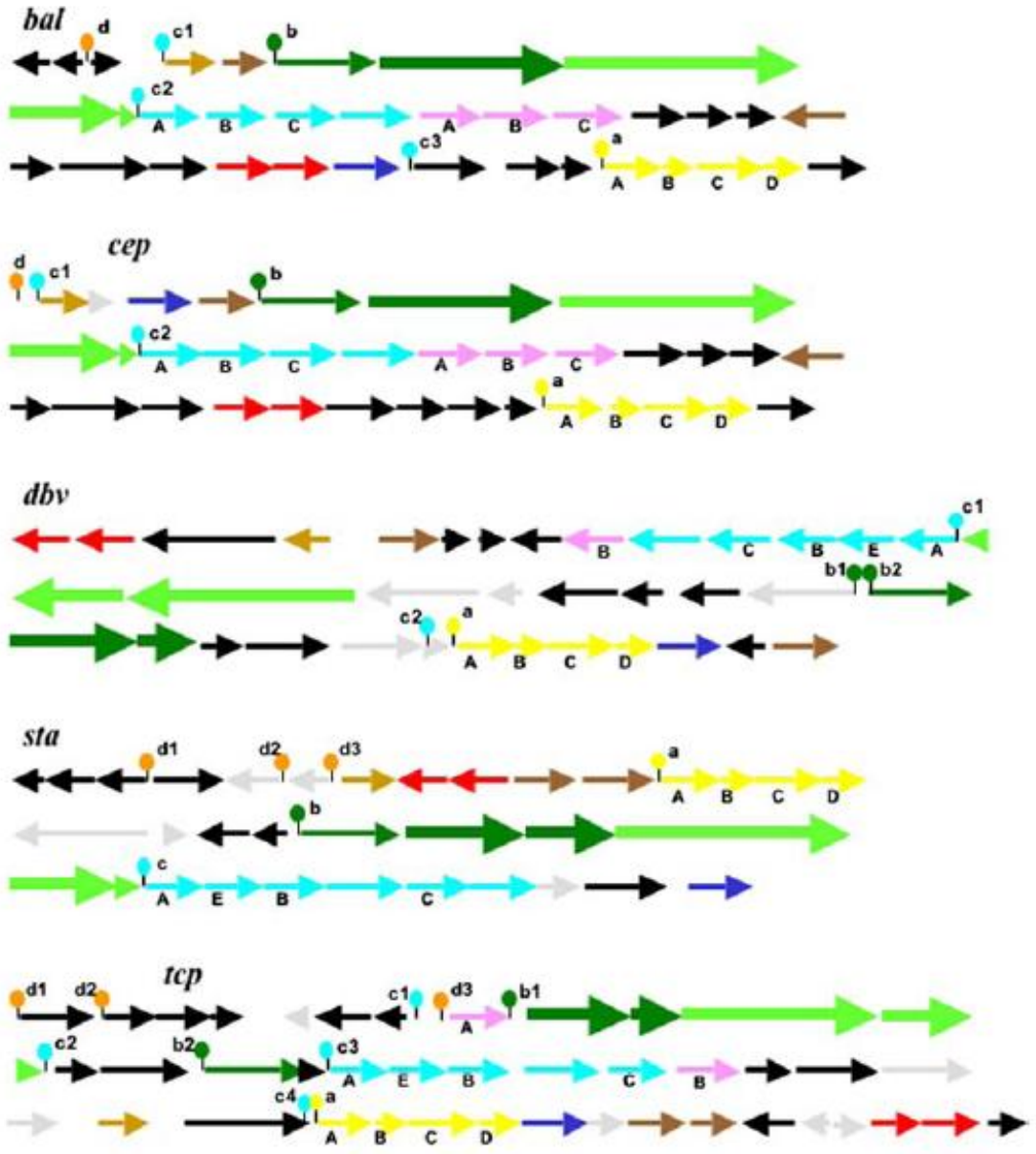

Fig. 11) Comparative analysis of balhimycin (*bal*), chloroeremomycin (*cep*), complestatin (*com*), A40926 (*dbv*), A47934 (*sta*), and teicoplanin (*tcp*) glycopeptides gene clusters. The genes present in each cluster are indicated by arrows drawn to scale, except in the case of the NRPS genes (thick arrows), which are drawn on a reduced scale. The segments of conserved synteny are identified by the color coding, and labeled with capital letters designating gene names: yellow, *dpgABCD*; light blue, *oxy-hal* region; pink, *gtf* region. Other colors indicate: red, *hmaS-hmo*; dark green, genes encoding the ABC transporter and NRPS modules 1 and 2; bright green, genes encoding NRPS modules 4–7 and the MbtH-like polypeptide; light brown, *strR*-like; dark brown, *hpgT* and the *prephenate dehydrogenase*-encoding gene; dark blue, the membrane ion antiporter gene. The black arrows denote genes shared by at least two clusters; while gray arrows refer to unique genes. Conserved IGSs (lower case letters) are symbolized by colored dots, as follows: yellow, dark green, light blue and orange indicate the conserved IGSs. (Donadio *et al.*, 2005).

All clusters contain an *strR*-like regulator gene (Table 1). StrR is a well-studied pathway-specific transcriptional regulator that activates the expression of streptomycin biosynthetic genes in *Streptomyces griseus* and *Streptomyces glaucescens*.

Biosynthetic role	Function[a]	Cluster[b]					Similarity (%)[c]	scores
		bal	*cep*	*dbv*	*Sta*	*tcp*		
Regulation	***StrR-like regulator***	1	1	1	1	1	52 (bt)	88 (bc)
	LuxR -like regulator			1		1		
	Sensor kinase	1[i]		1	1	1	37 (dt)	82 (st)
	Response regulator	1		1	1	1	59 (bd)	93 (st)

Table 1) Distribution of the regulator genes among the five glycopeptide clusters.

The phosphate-controlled regulator Dbv4 (StrR-like protein) is a cluster specific positive regulator and governs two key steps in A40926 biosynthesis: the biosynthesis of the non-proteinogenic amino acid 3,5-dihydroxyphenylglycine and critical tailoring reactions on the heptapeptide backbone (Alduina *et al*., 2007).

In particular, Dbv4 is a DNA-binding protein which acts as a regulator of A40926 biosynthesis by binding to the region upstream of *dbv14* and *dbv30* and likely controlling expression of two operons of the *dbv* cluster: the *dbv14-dbv8* operon, encoding the four cross-linking oxygenases, the halogenase, the *N*-acetylglucosamine transferase and the *N*-acylase, and the *dbv30-dbv35* operon, encoding the four enzymes involved in DPG biosynthesis, the sodium proton antiporter and a protein of unknown function.

Dbv4 was clearly unable to bind to its own upstream region. Similarly, the StrR-like regulator is not expected to control its own expression in the *tcp* clusters.

Furthermore, in experiments of affinity chromatography using as bait a DNA fragment upstream of the gene *dbv4* (called P4), a protein IclR-like was identified, that could have a role in regulating the expression of *dbv4* gene.

The *dbv3* genes (coding for a LuxR-like protein), *dbv6* (which encodes a putative response regulator, similar to VanR) and *dbv22* (which encodes a putative sensor regulator, similar to VanS) are localized in *dbv* gene cluster. Instead, the position of the *iclR* gene in *Nonomuraea* genome is not known.

Since poorly characterized in actinomycetes, the study of Dbv3, Dbv6, Dbv22 and IclR protein function could be especially interesting for understanding the mechanisms that govern metabolism and the morphological and physiological differentiation.

Dbv3: a Lux-R like protein

Among the clusters for the five glycopeptides, only A40926 and teicoplanin gene clusters contain a *luxR*-like gene (Table 1). Dbv3 belongs to LAL family (Large ATP-binding regulators of the LuxR family). The LuxR transcriptional regulator is a key player of a large variety of Quorum Sensing processes in many bacteria, regulating the expression of genes related to many processes such as antibiotic biosynthesis, motility, nodulation, plasmid transfer, bioluminescence, pathogenicity, biofilm formation.

The first example of LuxR protein was described in the marine bacteria *Vibrio fischeri*, where this protein is involved in a mechanism termed quorum sensing (Engebrecht *et al*., 1983; Fuqua and Greenberg, 2002; Yang *et al*., 2009). Quorum sensing is the process by which bacteria communicate with one another using chemical signal molecules; a large group of cells can synchronize its activity responding to hormone-like molecules, acting as a multi-cellular organism. Bacteria can secrete signal molecules called autoinducers (AIs), that allow to monitor their own population density.

Vibrio fischeri lives in symbiotic association with a number of eukaryotic hosts that developed a specialized light organ that is inhabited by a pure culture of a specific strain of *V. fischeri* at very high cell density (Fig. 12). In these symbiotic associations the eukaryotic host supplies *V. fischeri* with a nutrient-rich environment in which to live. The role of *V. fischeri* is to provide the host with light used as anti-predation strategy (illumination enables the squid to avoid casting a shadow beneath it on bright clear nights when the light from the moon and stars penetrates the seawater) or the luminescent regions on the fish are apparently seductive to fish of the opposite sex.

When these bacteria are cultured in broth, they exhibit a lag in luminescence gene (*lux*) expression during early and mid-exponential growth, followed by a rapid increase in expression during the late exponential and early stationary growth phases. At low cell

density, LuxI produces AI (3oxo-C6- homoserine lactone) that is not accumulated in the environment. At high cell density, when AI concentration reaches a threshold concentration, it enter into cells and forms an active complex with LuxR; this complex binds to specific promoter sequences called lux-boxes controlling the transcription of *lux* operon.

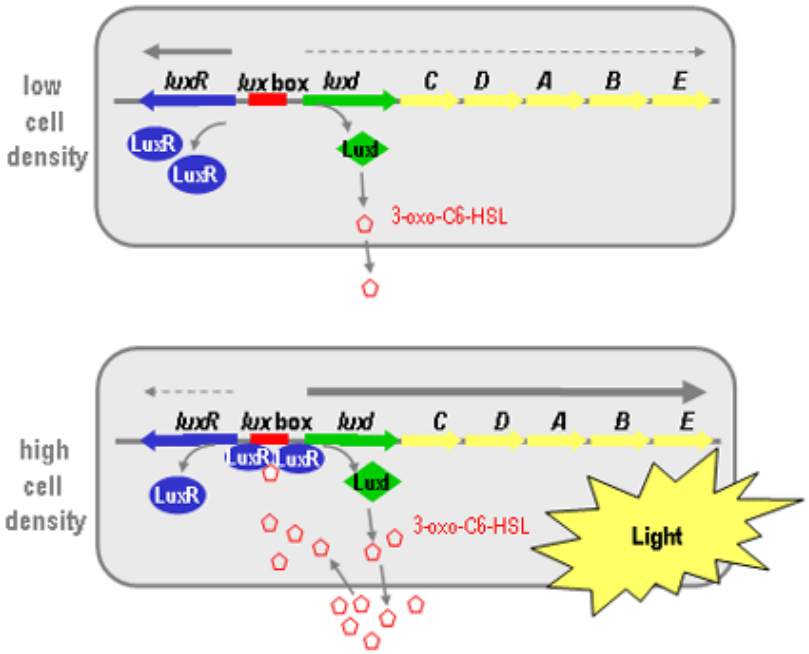

Fig.12) The *V. fischeri* luminescence genes are organized in two divergently transcribed units with an intergenic region of about 250 bp. One unit contains *luxR*, which encodes the 250-amino-acid LuxR transcriptional activator. The other unit is a 7 genes-operon, *luxICDABEG*: *luxI* encodes a protein that synthesizes the autoinducer (3oxo-C6-homoserine lactone); the other genes play mechanistic roles in light production.

The production of antibiotics in some *Streptomyces spp*. depends upon diffusible butyrolactones structurally similar to homoserine lactones. The most intensively studied is the A factor; it is gradually produced by AfsA and accumulated in a growth dependent manner (Horinouchi *et al.*, 1994). When the concentration of A-factor reaches a critical level at or just before the decision point, it binds an A factor-specific receptor, ArpA, which has bound and repressed the promoter of *adpA*, and dissociates ArpA from the promoter, thus leading to *adpA* transcription and translation. The transcriptional activator

AdpA then activates a variety of genes that are required for the biosynthesis of secondary metabolites, including streptomycin, and morphological differentiation in *Streptomyces griseus* (Fig.13).

In general, butyrolactone-mediated regulation appears similar to autoinducer-dependent regulation, but the two systems are actually quite distinct. While LuxR-type proteins activate transcription, the A-factor receptor is a repressor that is neutralized by A factor.

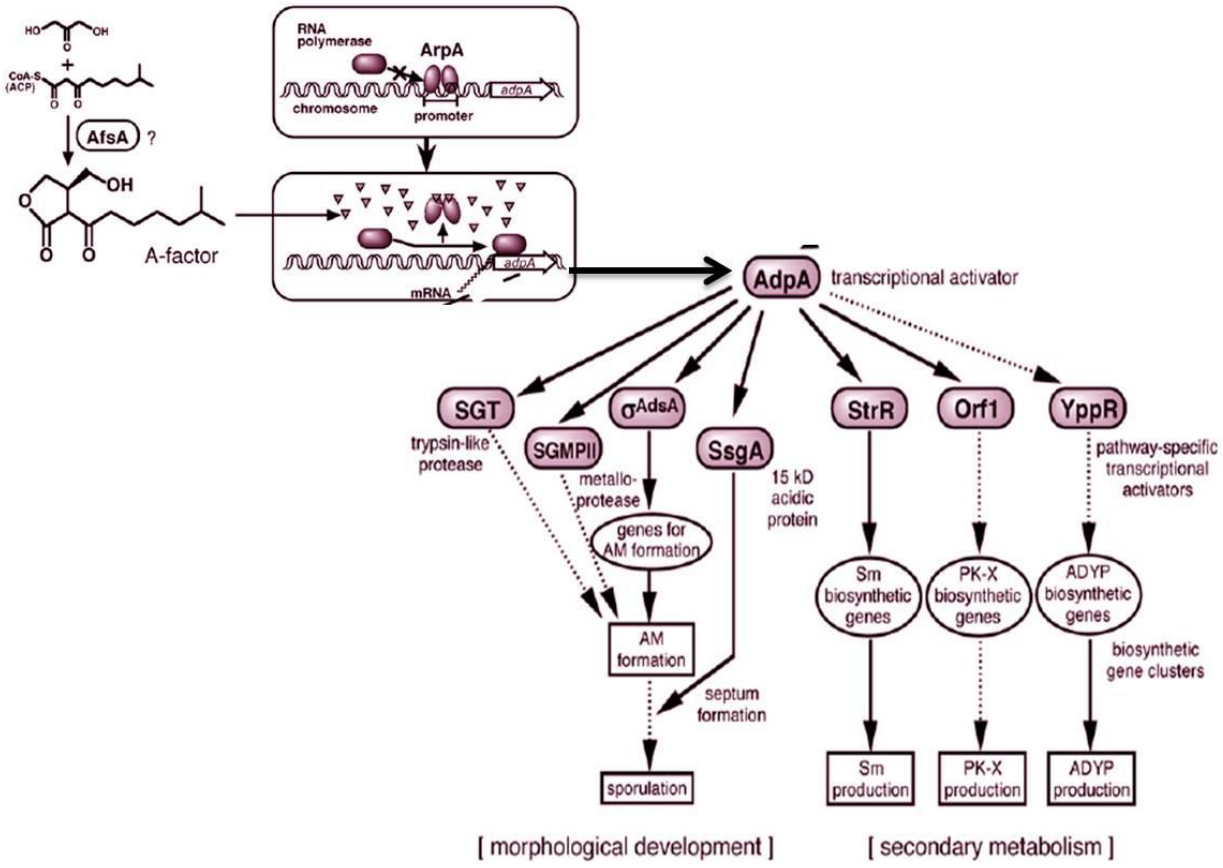

Figure 13). The A-factor regulatory cascade in *S. griseus*.

In the model *S. coelicolor* the protein ScbR2, homologue of γ-butyrolactone (GBL) receptor, is shown not to bind the endogenous GBL molecule SCB1; intriguingly, it could bind the endogenous antibiotics actinorhodin and undecylprodigiosin as ligands, leading to activation of a cryptic type I polyketide synthase gene cluster (Fig. 14).

Likewise, JadR2 is also a putative GBL receptor homologue in *Streptomyces venezuelae*. When JasR2 binds cloramphenicol and jadomycin, it derepresses *jadR1*: JadR1 activates jadomycin biosynthesis and represses chloramphenicol biosynthesis (Xu *et al.,* 2010). Antibiotics are known to have a general signaling role to induce global changes in gene transcription in a bacterial community; moreover, like quorum sensing molecules, antibiotics can also act as intracellular signals to induce downstream responses thanks to GBL receptors.

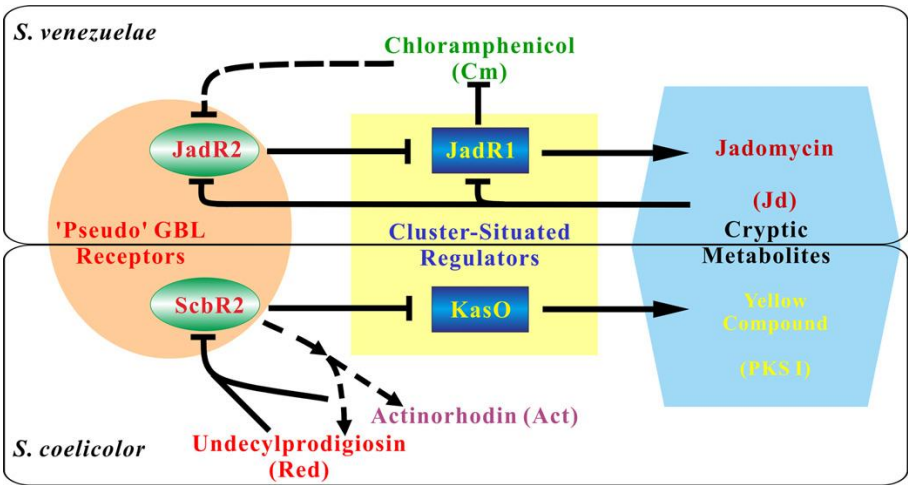

Fig.14) Cross coordination of different antibiotic biosynthesis by pseudo GBL receptors

Two *S. coelicolor* LAL proteins were recently found to positively regulate the production of blue pigmented polyketide actinorhodin (Act) and globally affect various cellular processes, i.e. both regulators are involved in the phosphate starvation response (Guerra *et al.* 2012).

In *silico* analysis shows that Dbv3 is a LuxR like protein of 867 amino acids composed by two domains (Fig.15). The C-terminal DNA-binding domain of Dbv3 contains a helix-turn-helix motif. Indeed, proteins belonging to this group are response regulators; some act

as transcriptional activators, others as transcriptional repressors. A dimerization interface is present in the C-terminal domain. The Dbv3 N-terminal region contains a putative P-loop NTPase superfamily domain. This family of regulators is characterized by the unusual size of its members. The P-loop NTPase domain hydrolyses the β–γ phosphate bond of a bound nucleoside triphosphate (often ATP or GTP) and utilizes the free energy of NTP hydrolysis to induce conformational changes in other molecules.

Fig.15) Dbv3 conserved domains

Dbv6 and Dbv22: a two component system

Dbv6 is a protein VanR-like, while Dbv22 could be the sensor on the membrane. VanS and VanR are an example of a two-component system, identified in pathogenic bacteria resistant to the glycopeptide vancomycin (Hong, *et al* 2008). In *S. coelicolor* it has been shown that VanS and VanR activate the transcription of *vanHAX* genes, for resistance to the glycopeptide antibiotic vancomycin (Fig. 16). The presence of VanR / VanS in many microorganisms producing glycopeptides and not, led to hypothesize a broader role possibly associated with morphological differentiation.

In *Nonomuraea vanHAX* genes are not present but it has the *vanY* gene, which encodes a carboxypeptidase able to cut the D-alanyl-D-alanine end (D-Ala D-Ala) of the peptidoglycan precursor outside the cell membrane. VanY is a novel protein involved in the mechanism of self-resistance in *Nonomuraea* sp. ATCC 39727. VanY (196 residues) is encoded by the *dbv7* gene within the *dbv* biosynthetic cluster devoted to A40926 production.

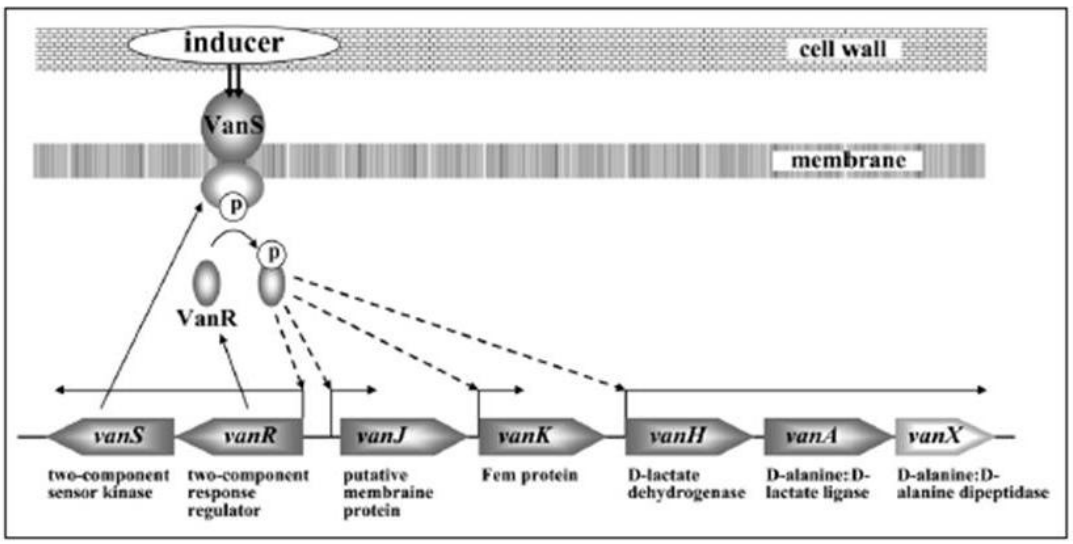

Fig. 16) Mechanism of action of VanR-VanS in *S. coelicolor* (Hong *et al.*, 2005)

The analysis of the sequence suggests the presence of a hydrophobic transmembrane portion and two conserved sequences (SxHxxGxAxD and ExxH) in the extracytoplasmic domain that are potentially involved in coordination of $Zn^{(2+)}$ and catalytic activity. The presence of these conserved sequences indicates a similar mechanism of action and substrate binding in VanY as in VanY, VanX and VanXY $Zn^{(2+)}$-dependent D,D-carboxypeptidases and D-Ala-D-Ala dipeptidases acting on peptidoglycan maturation and involved in glycopeptide resistance in pathogens (Binda *et al.*, 2012). A recent work indicated that the minimum inhibitory concentration (MIC, that is the lowest concentration of an antimicrobial that inhibits the visible growth of a microorganism after overnight incubation) of *Nonomuraea* sp. ATCC 39727 towards A40926 during vegetative growth was 4 g/ml, but this increased to ca. 20 g/ml during A40926 production (Marcone *et al.*, 2010). This result indicated that resistance to A40926 is regulated by A40926 production.

IclR

Members of the IclR family are proteins of around 250 residues. These regulators have a helix-turn-helix DNA binding motif in the N-terminal domain and bind target promoters as dimers or as a dimer of dimers.

This family comprises regulators acting as repressors, activators and proteins with a dual role. In *E. coli* IclR uses two modes of repression. The repression mode I involves IclR bound to its target site overlapping RNA polymerase binding site, so that occupancy of the site by IclR prevents the entry of the polymerase. The repression mode II involves IclR bound to a distal site with respect to the RNA polymerase site. The interaction of IclR with the α-subunit of the promoter-bound RNA polymerase destabilizes and disassociates the open complex (Yamamoto & Ishihama, 2003, fig. 17). IclR-type positive regulators bind promoter DNA in the absence of effectors.

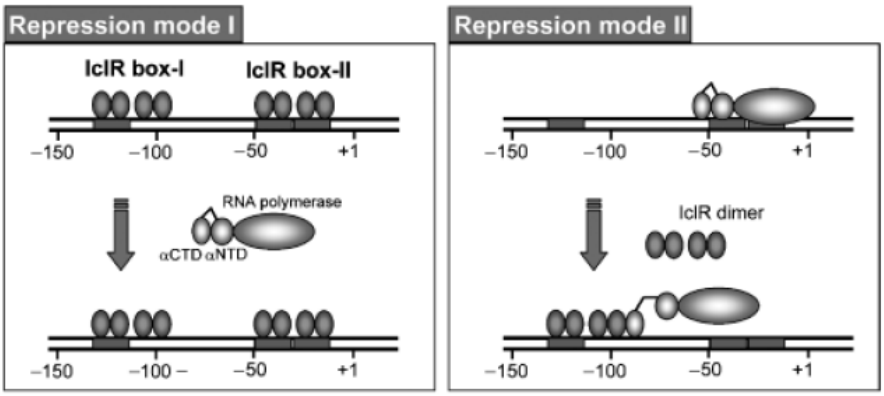

Fig 17) Modes of repression of IclR in *E. coli* (Molina-Henares *et al.*, 2004)

Members of the IclR family have pleiotropic roles (Fig.18) and control genes, whose products are involved in the glyoxylate shunt, multidrug resistance, degradation of aromatics, inactivation of quorum-sensing signals, determinants of plant pathogenicity and sporulation. In *S. coelicor ssgR* facilitates the sporulation via SsgA, factor that is involved in sporulation and morphogenesis (Traag *et al.*, 2004).

IclR family members also control bacterial adaptation to the fluctuation of environment, regulating efflux pumps to exclude toxic substances. For example, TtgV of *Pseudomonas putida* is an IclR repressor of *ttgGHI* operon encoding pumps empowering bacterial higher resistance to toluene. IclR-like AttJ regulates stability of quorum sensing signals in *Agrobacterium tumefaciens.*

LtbR in *C. glutamicum* negatively controls *leuB, leuC* and *trpE* involved in the production of leucine and tryptophane.

In *S.coelicolor* GylR is responsible of glycerol catabolism: in fact GylR is the repressor of the *gylCABX* operon and it also acts as a negative autoregulator (Zhou *et al*., 2012).

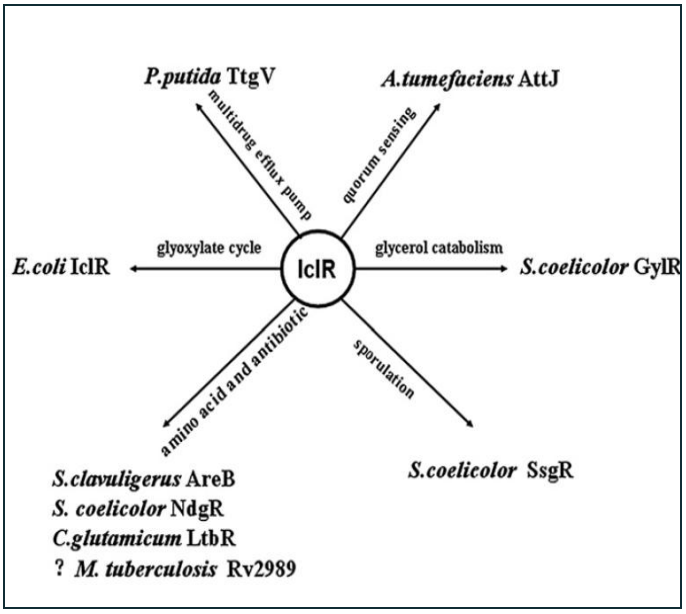

Fig.18) Pleiotropic role of IclR family among bacteria (Zhou *et al.,* 2012)

AreB in *Streptomyces clavuligerus* activates transcription of *leuCD* operon involved in leucin biosynthesis (Santamarta *et al*., 2007). Therefore, AreB controls cephamycin C and clavulanic acid production and fatty acid catabolism (Fig.19,a). In *S. coelicolor* NdgR positively controls leucin biosynthesis, negatively controls actinorhodin and undecilprodigiosin production; it is also involved in quorum sensing mechanism (Fig.19, b). Deletion mutants in *ndgR* showed poor growth in a defined minimal medium and

supplementation of cysteine and methionine corrected growth, suggesting that NdgR induced cysteine-methionine biosynthesis (Kim *et al*., 2012).

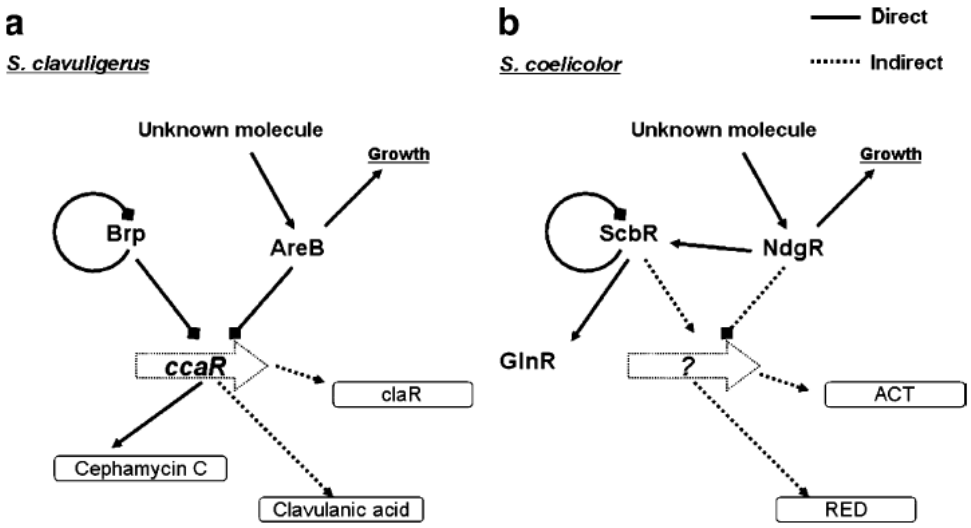

Fig.19) Role of IclR family in *S. clavuligerus* and *S. coelicolor* (Kim *et al*., 2012).

Bacteria have developed sophisticated mechanisms to adapt to environmental changes. For example, carbon catabolite repression (CCR) allows bacteria the assimilation of a preferred (i.e. rapidly metabolisable) carbon source when they are exposed to more than one carbohydrate. CCR is a complex regulatory phenomenon frequently mediated via several mechanisms. This is usually achieved through inhibition of synthesis of enzymes involved in catabolism of carbon sources other than the preferred one. The catabolite repression was first shown to be initiated by glucose and therefore sometimes referred to as the glucose effect.

During aerobic growth of *Escherichia coli* on acetate as sole source of carbon and energy, the organism requires the operation of the glyoxylate bypass enzymes, namely isocitrate lyase (ICL) and the anaplerotic enzyme malate synthase (MS) and this mechanism is under control of an IclR protein (Fig.20). Under these conditions, the glyoxylate bypass enzyme ICL is in direct competition with the Krebs cycle enzyme isocitrate dehydrogenase (ICDH)

for their common substrate and although ICDH has a much higher affinity for isocitrate, flux of carbon through ICL is assured by virtue of high intracellular level of isocitrate and the reversible phosphorylation/inactivation of a large fraction of ICDH.

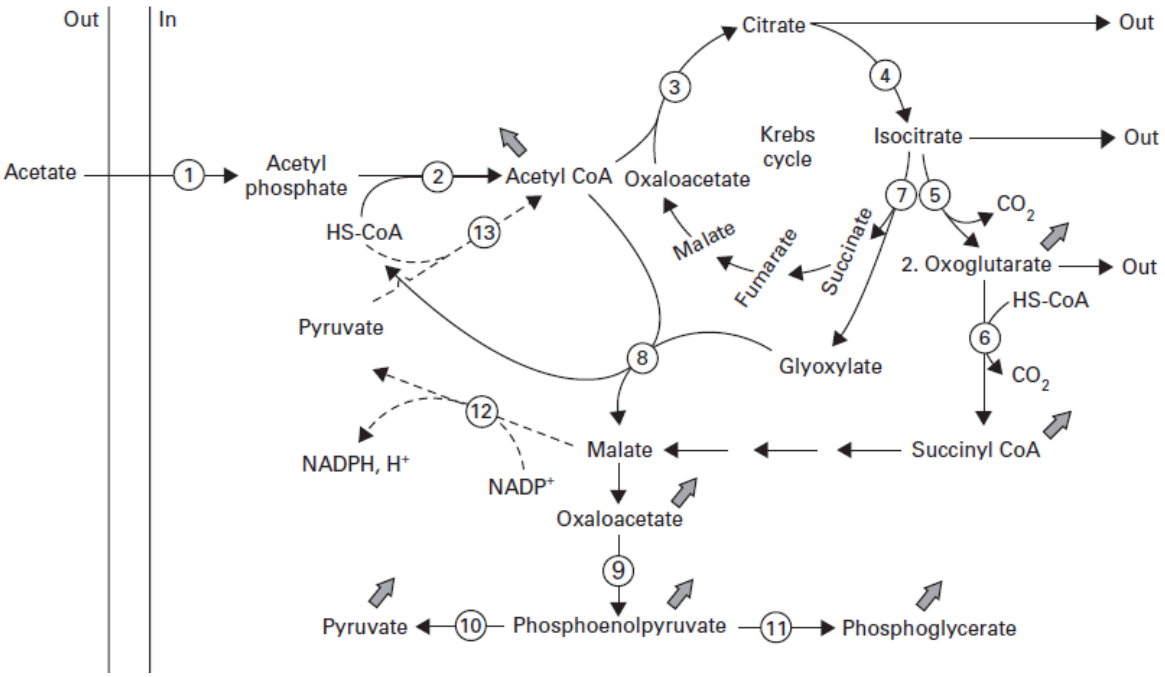

Fig.20) Schematic representation of the metabolic routes employed by *E. coli* for acetate metabolism, highlighting the direct competition between glyoxylate bypass enzyme and the Krebs cycle isocitrate dehydrogenase for their common substrate (isocitrate). Enzymes are: 1=acetate kinase; 2=phosphotransacetylase; 3=citrate synthase; 4=aconitase; 5=isocitrate dehydrogenase; 6=αchetoglutarate dehydrogenase; 7=isocitrate lyase; 8=malate synthase; 9=phosphoenolpyruvate carboxykinase; 10=pyruvate kinase; 11=enolase; 12=malic enzyme; 13=pyruvate dehydrogenase.

Reversible inactivation is due to reversible phosphorylation catalysed by ICDH kinase/phosphatase, which harbors both catalytic activities on the same polypeptide. The structural gene encoding ICDH kinase/phosphatase *(aceK)* together with those encoding ICL *(aceA)* and MS *(aceB)* form an operon (*aceBAK*; otherwise known as the *ace* operon) whose expression is intricately regulated at the transcriptional level by several regulators, i. e. IclR, FadR, FruR and IHF. Conversely, when bacteria are cultured on carbon sources,

such as glucose or glycerol, which do not employ the glyoxylate bypass as an anaplerotic sequence, IDH is not phosphorylated and remains fully active. The *ace* operon is subjected to repression at the transcriptional level by IclR (Cozzone *et al.,* 2005).

The IclR binding site of *aceBAK* is AAAATGGAAATTGTTTTTG, while for *iclR* self-regulation is AAAATGAAAATGATTTCCA (Zhou *et al*. 2012). In *E. coli,* IclR repressor shows that, among various molecules (Acetate, acetyl-CoA, pyruvate, phosphoenol pyruvate and oxaloacetate), only phosphoenol pyruvate appeared to prevent the formation of the IclR-DNA complex (Cortay *et al*.1991).

In *S. coelicolor* the *gyl* operon for glycerol catabolism is a polycistronic transcript contains four genes collectively termed *gylCABX*. The first three genes encode a putative glycerol transporter, a glycerol kinase, and a glycerol-3-phosphate dehydrogenase, while *gylX* encodes a gene of unknown function (Smith *et al.*, 1988). The *gyl* operon is transcribed from two closely spaced glycerol-inducible and glucose-repressible promoters, named gylP1/P2. Glycerol induction and glucose repression of gylP1/P2 are probably mediated by the glycerol-inducible repressor GylR (an IclR like protein), whose encoding gene locates immediately upstream of the *gylCABX* operon. GylR controls the expression of both *gylR* and *gylCABX* (Hindle *et al.*, 1994). Null mutations into the chromosomal *gylR* gene demonstrated that GylR is the repressor of the *gylCABX* operon and also revealed that GylR functions as a negative autoregulator. Substrate induction and catabolite repression of *gyl* are mediated through the GylR protein. This is the first direct evidence that catabolite repression in *Streptomyces* is not exerted at the transcriptional level by a general 'catabolite repressor protein'.

In the vast majority of documented cases, the preferred carbon source is glucose with the famous *Escherichia coli* glucose/lactose classical example (Inada *et al.*, 1996). On the

contrary, the lactic acid bacterium *Streptococcus thermophilus* prefers lactose over glucose (van Den Bogaard *et al.*, 2000), indicating that adaptation to special ecological niches may result in the choice of practically any carbohydrate as favored substrate.

To my knowledge, the preferred carbon sources and the carbon catabolite repression mechanisms have not yet been studied in *Nonomuraea*.

Moreover, up to now no role was assigned to IclR in *Nonomuraea*.

Aim of the project

Actinomycetes are producers of a wide variety of bioactive secondary metabolites but wild-type bacteria often produce desired metabolites at low yield; thus, high production strains are always needed for commercial use. Classical strain improvement methods depend on iterative rounds of random mutagenesis on parental strain with subsequent large-scale screening of mutants to identify high-producing strains. Although the strategy was successfully applied in the fermentation industry for a long time, it is labor intensive, and the improved could not be easily understood. The establishment of genetic engineering technology for actinomycetes makes rational strain improvement possible (Chater, 1990). Over-expression of positive regulatory genes or disruption of negative regulatory genes were commonly adopted as the first step to verify the function of regulatory genes and to generate overproduction strains.

My research aimed to broaden understanding the mechanisms of regulation of physiological differentiation and gene expression in Actinomycetes.

In particular, the purpose of this research was to study the role of *dbv3*, *dbv4*, *dbv6*, *dbv22* and *iclR* genes and their involvement in morphological and physiological differentiation in *Nonomuraea*.

Results

Construction of *Nonomuraea* mutants deleted in *dbv3, dbv4, dbv6* and *dbv22* genes

To investigate the role of regulatory genes of A40926 production, Ko *dbv3,* Ko *dbv4,* Ko *dbv6 and* Ko *dbv22* strains were constructed by replacing the wild-type gene with an in vitro generated allele interrupted by insertion of apramycin resistance cassette (Redirect technology). Double-crossover mutants were screened by apramycin resistance. The putative mutants were analyzed by PCR. For Ko *dbv4, a* PCR product of 1,8 Kb was obtained for the clone 4.9, 4.10 and clone 4.11 among the putative eleven exconjugants, while wild type gave a PCR product of 1,3 kp (lane 4.1-4.7 and 4.12; Fig. 21).

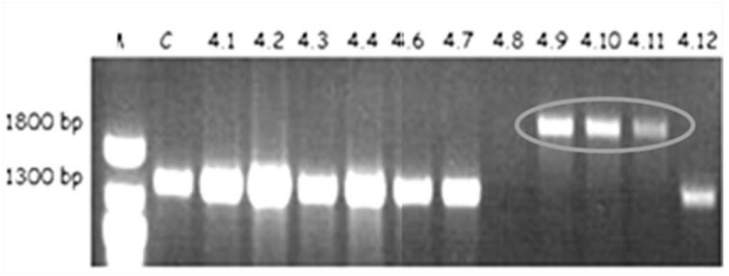

Fig 21) PCR of putative Ko *dbv4* mutants. PCR product of the mutant is indicated by a circle. C: positive control.

For Ko *dbv3, a* PCR products of 1,8 kb was obtained for a clone (lane 4) among four putative exconjugants, while wild type gave a PCR product of 2,8 kb (lane 6, Fig. 22).

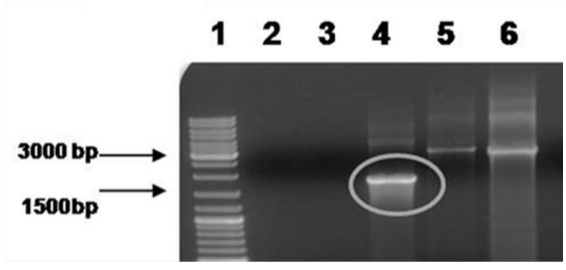

Fig. 22) PCR of putative Ko *dbv3* mutants. PCR product of the mutant is indicated by a circle. lane 6: positive control.

For Ko *dbv6, a* PCR products of 1,5 Kb was obtained for a clone (lane 9) among seven putative exconjugants, while wild type gave a PCR product of 8oo bp (lane 10, Fig. 23).

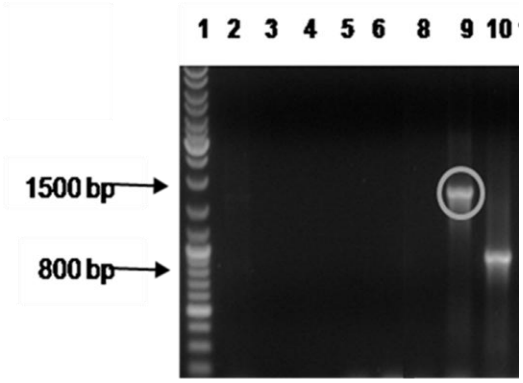

Fig. 23) PCR of putative Ko *dbv6* mutants. The PCR product is indicated by a circle. lane 10: positive control.

For Ko *dbv22, a* PCR products of 1,7 kb was obtained for a clone (lane 2) among ten putative exconjugants, while wild type gave a PCR product of 1,5 Kb (lane 1, lane 3-12. Fig. 24).

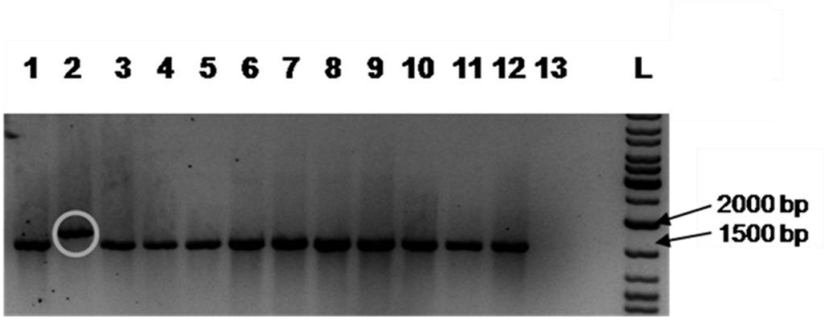

Fig. 24) PCR Ko *dbv22* mutants. The PCR product is indicated by a circle. Lane 1: positive control.

Sequencing of PCR products demonstrated that the apramycin-resistant cassette was correctly inserted in the target genes through homologous double-cross recombination.

Role of *dbv3, dbv4, dbv6* and *dbv22* on A40926 biosynthesis

Disruption of *dbv3, dbv4, dbv6* and *dbv22* genes did not significantly alter growth kinetics. In fact, the mutants showed the same growth rate and morphological characteristics as the parental strain on several media (i.e. R3, MS, V01 solid media, or R3 liquid medium) indicating that the *dbv3, dbv4, dbv6* and *dbv22* genes are not critical for bacterial growth and differentiation.

Interestingly, microbiological assays showed that Ko *dbv3* and Ko *dbv4* mutants lost the capacity to produce antibiotic while, wild type produced A40926 from 72 hours of growth. HPLC assays confirmed that no A40926 was produced by the two mutant strains. These results showed that Dbv3 and Dbv4 positively control A40926 biosynthesis and they are necessary for antibiotic production.

Instead, *dbv6* and *dbv22* are not involved in A40926 biosynthesis; in fact in *dbv6* and *dbv22* mutants antibiotic production was not affected in the rich R3 broth.

Dbv6 and resistance to A40926

To evaluate a possible relationship between VanS / VanR like system and resistance to the antibiotic, resistance assays have been conducted. *Nonomuraea* wild type and Ko *dbv6* mutant were grown in SM liquid medium for 48 hours, at which time it was ascertained the presence of an exponential phase of growth and lack of antibiotic production. Ko *dbv3* mutant was used as control strain. Each strain was seed on SM plate in order to obtain confluent culture. Sterile absorbent paper disks were soaked with various concentrations of the glycopeptide antibiotic vancomycin (25 , 12.5 , 5 and 3.5 µg), which is similar in structure and mechanism of action to A40926 (which is not available as pure powder). For each plate four paper disks well spaced were arranged. After 72 h of growth at 30°C, we observed that in presence of 25 µg of vancomycin the three strains are equally sensitive, while at 12.5, 5 and 3.5 µg both wild-type and Ko *dbv3* mutant are more resistant than Ko*dbv6* mutant, for which the zone of inhibition was larger (Fig. 25).

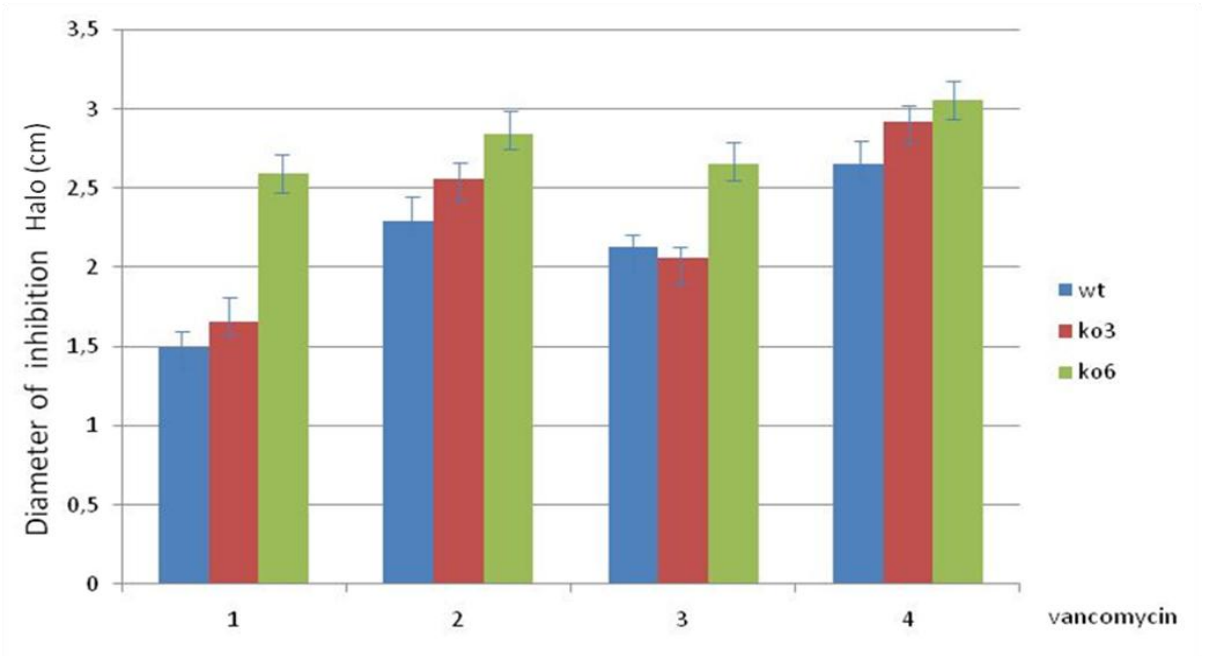

Fig 25) Resistance assays to vancomycin of *Ko dbv3, Ko dbv6* and wild type.
Concentration of vancomycin 1) 3.5 µg, 2) 12.5 µgl; 3) 5 µg, 4) 25 µg.

To confirm this result, an other resistance assay on plate was carried out, to measure the minimum inhibitory concentration (MIC) of antibiotic for the bacterium (Fig.26). In each SM plate the following amount of Vancomycin was added: 0 - 0,5 - 1,25 - 2,5 – 5 - 12,5 - 25 μg/ml respectively and subsequently, a dense bacterial suspension was seed on the plates. After 72 hours at 30° C, the Ko *dbv6* strain did not grow starting from 1.25 mg / ml of vancomycin (MIC), while some colonies of wild-type grew in presence of 12.5 mg / ml of vancomycin.

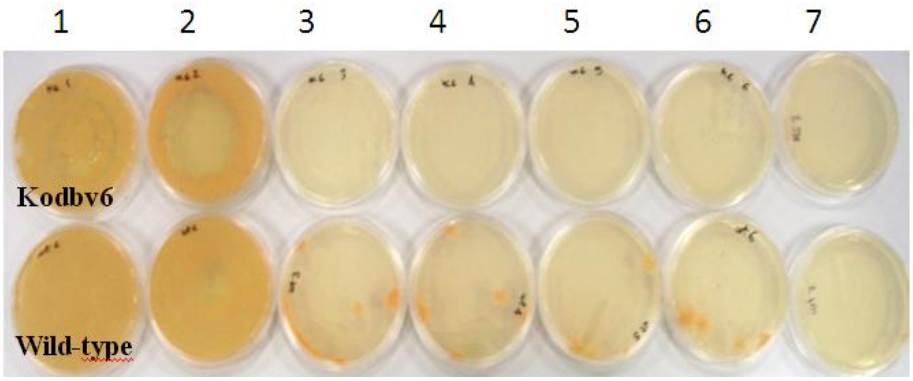

Fig 26) Resistance assays to vancomycin of *Ko dbv6* and wild type. Concentration of vancomycin 1) 0 mg /ml; 2) 0.5 mg /ml, 3) 1.25 mg / ml, 4) 2.5 mg / ml, 5) 5 mg / ml, 6) 12.5 mg / ml; 7) 25 mg / ml.

Both results suggest that Dbv6 could be positively involved in the regulation of resistance to glycopeptides. Further analysis are necessary to confirm these hypothesis.

Dbv3 and Dbv4: Transcriptional control of A40926 production

Dbv4 was previously shown to bind the upstream region of *dbv14* and *dbv30* genes and to control expression of the *dbv14-dbv8* and *dbv30-dbv35* operons (Alduina *et al*., 2007). Indeed, RT-PCR analysis showed that *dbv14* is not transcribed in the Ko *dbv4* mutant incubated in R3 for 48h. To understand the hierarchy between *dbv3* and *dbv4*, RT-PCR analysis of *dbv3* was carried out using RNA extracted from Ko *dbv4* mutant. This analysis revealed that *dbv3* is transcribed, demonstrating that Dbv4 does not control *dbv3* transcription (Fig. 27).

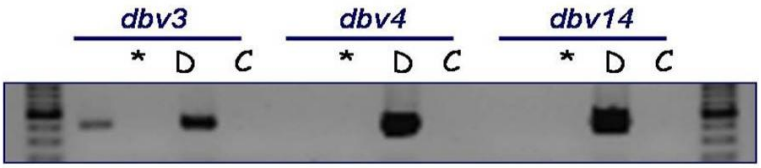

Fig. 27) RT-PCR analysis of Ko *dbv4* RNA using primers for *dbv3*, *dbv4* and *dbv14* genes. D: positive control (DNA); C: negative control (water); *: negative control (-RT).

On the other hand, *dbv4* is not transcribed in Ko *dbv3* mutant grown in R3 for 48 and 72h, suggesting a control of Dbv3 on *dbv4* transcription (Fig. 28). As a consequence, neither *dbv14* nor *dbv30* are transcribed in ko *dbv3* mutant.

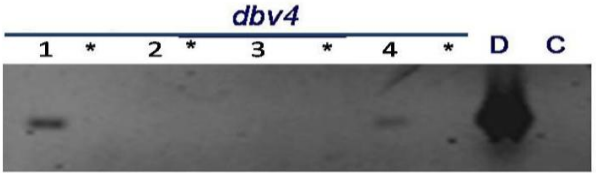

Fig 28) RT-PCR analysis of *dbv4* gene transcription using RNA from wild type (lane1), Ko *dbv3* (lane2) Ko *dbv4* (lane3) and ko *dbv6* (lane 4) mutants.
D: positive control (DNA); C: negative control (water); *: negative control (-RT).

Moreover, qRT-PCR of some *dbv* genes revealed that in the Ko *dbv3* mutant transcript levels of *dbv* genes are six - ten fold lower than in wild type (Fig. 29).

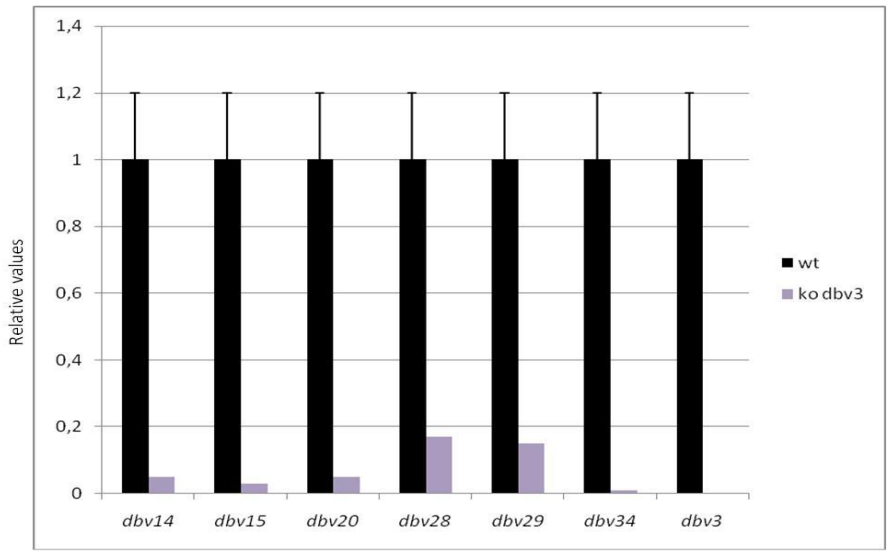

Fig. 29) qRT-PCR of some *dbv* genes in Ko *dbv3* mutant.

Construction of *dbv3* over expression mutant

Analysis conducted on the Ko *dbv3* mutant suggested that Dbv3 controls transcription of the positive pathway specific regulator Dbv4. Global or pathway-specific regulatory factors can be exploited to enhance the production of secondary metabolites. To this end, a *Nonomuraea* strain that over-expresses *dbv3* was constructed. pIJ8600, an integrative plasmid for Actinomycetes, was used to add a copy of the *dbv3* gene in the neutral *attB* site of bacterial chromosome. The genomic integration of pIJ8600-*dbv3* in the mutant was verified by PCR and Southern blot analysis (Fig. 30). The genome of *Nonomuraea* has not yet been sequenced. After hybridization using pIJ8600 digested with *PstI* as probe two bands of hybridization (about 4,3 and 3,9 kb, lane 1) and four bands (about 6 kb, 4,3 kb, 2 kb, 800 bp, lane 2) were obtained, as expected. No hybridization signal was detected for *Nonomuraea* wild type (lane 3 and 4).

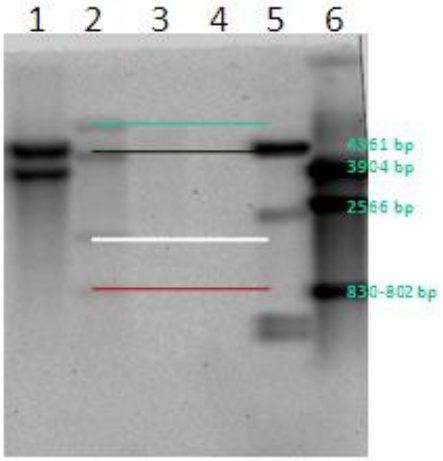

Fig. 30) Southern hybridization of over *dbv3* mutant using pIJ8600 digested with *PstI*. Lane 1: Ko *dbv3* mutant chromosomal DNA digested with *BamHI; lane 2:* over *dbv3* chromosomal DNA digested with *PstI; lane 3:* wild type chromosomal DNA digested with *BamHI; lane 4:* wild type chromosomal DNA digested with *PstI*; lane 5: marker II; lane 6: pIJ8600 digested with *PstI*.

A control strain that contains a copy of the empty plasmid was generated. Six clones, named 1, 22, 35, 36, 52 and 68, were obtained. The genomic integration of pIJ8600 was verified by PCR and Southern blot analysis (Fig.31). After hybridization using pIJ8600 digested with *PvuII* as probe three bands of hybridization were obtained, as expected, in the case in which the mutant DNA had been digested with *PvuII* (lane 3-8). No hybridization signal was detected for *Nonomuraea* wild type (lane 2).

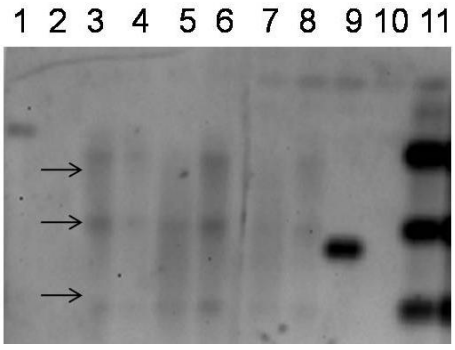

Fig.31) Southern hybridization of *Nonomuraea*::pIJ8600 ex-conjugant using *PvuII* digested pIJ8600 as probe. Lane 1 Marker 2; genomic DNA digested with *PvuII* of wild type (Lane 2), and *Nonomuraea*::pIJ8600 clone 1 (lane 3), clone 22 (lane 4), clone 35 (lane 5), clone 36 (lane6), clone 52 (lane 7), clone 68 (lane 8); lane 9: 1 kb ladder; lane 11: *PvuII* digested pIJ8600.

To value the effect of pIJ8600 integration in *Nonomuraea* chromosome on A40926 production, microbiological assays of *Nonomuraea*::pIJ8600 ex-conjugants were performed (Fig.32). The analysis revealed that, in respect to the wild type, four ex-conjugants produced the same amount of antibiotic (clones 35, 36, 46, 49, 68); one produce more antibiotic (clone 22) but standard deviation indicated that this result is not significant; one (clone 52) produced lower amount of antibiotic.

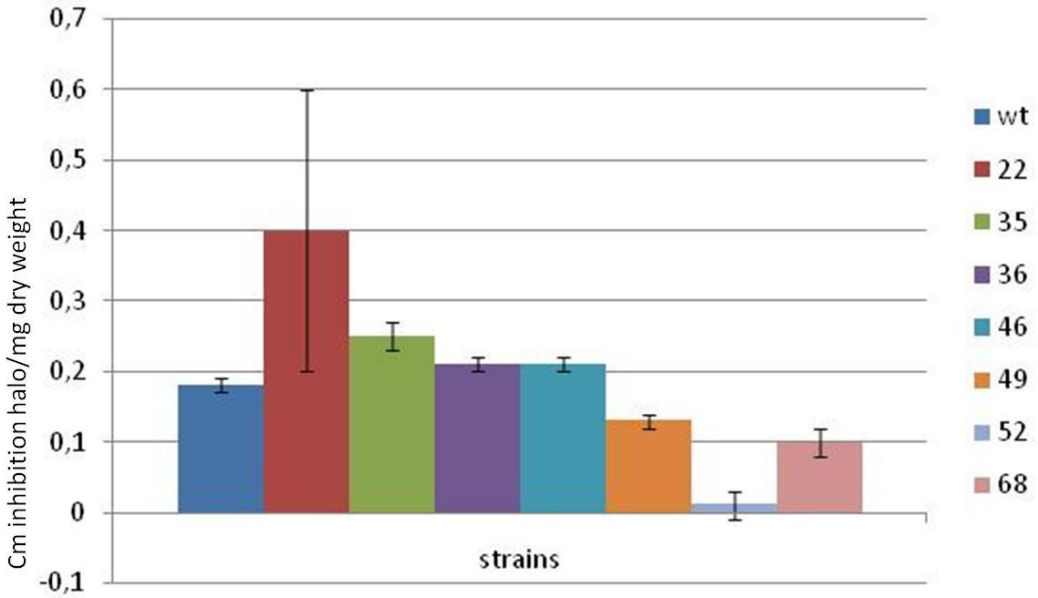

Fig. 32) Antibiotic production of wild type and *Nonomuraea*::pIJ8600.

Overexpression of *dbv3* increases A40926 production

In agreement with results obtained with Ko *dbv3* mutant, growth of *Nonomuraea* wild type and over *dbv3* mutant in the complete liquid medium R3 is similar: there is a rapid growth phase until 72 hours, then a decrease until 140 hours. There is a second growth with a peak at 202 hours for wild type and over *dbv3* and then the decline phase.

Microbiological assays showed that wild type begins to produce A40926 at 72 hours, while over *dbv3* mutant at 54 hours. Moreover, diameter of the inhibition halo was greater in the mutant strain compared to the wild type, indicating a higher production of A40926 by over *dbv3* mutant in respect to wild type. So, *dbv3* over expression anticipated and increased antibiotic production. In fact productivity, that is the ratio between µg of antibiotic, ml of culture and dry weight (grams), was 1,6 fold higher in over *dbv3* mutant than in the wild type (Fig.33). HPLC confirmed that over *dbv3* mutant produced about 2 fold more A40926 than the wild type strain.

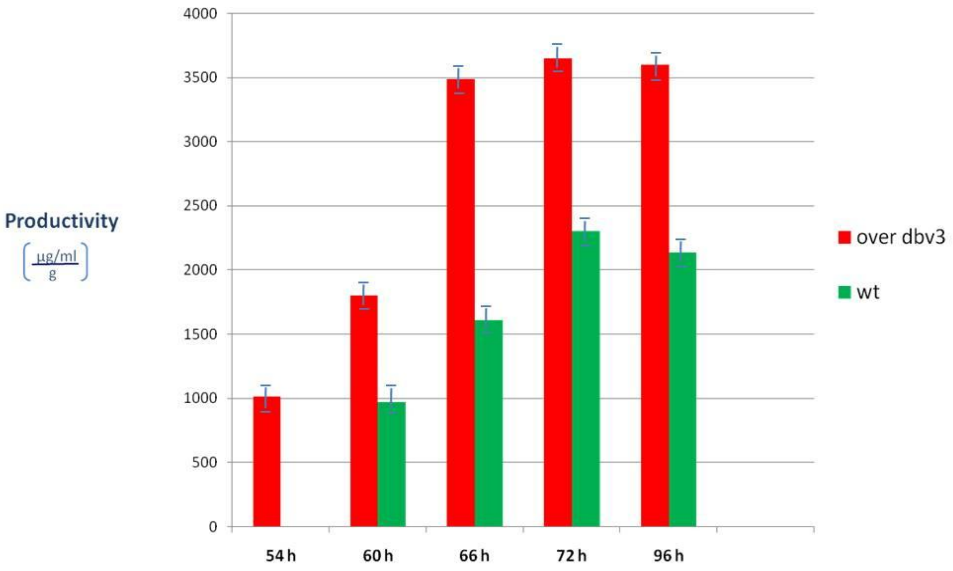

Fig. 33) Productivity of *Nonomuraea* over-*dbv3* and wild type after 54, 60, 66, 72 and 96 hours of growth in liquid R3.

Dbv3: transcriptional control of A40926 production

Dbv3 plays a positive role in A40926 production. To evaluate whether Dbv3 acts through the activation of the *dbv* cluster, wild type and over-*dbv3* mutant were incubated with and without thiostrepton (tio), used as inducer of *dbv3* transcription from the TipA promoter in the mutant strain. RNAs were extracted from after 54 hours of growth and analysed by qRT-PCR.

qRT-PCR analysis revealed that the addition of thiostrepton did not affect *dbv3* transcription level in wild type (Fig. 32, see wt and wt + tio transcript levels); moreover, in over *dbv3* mutant *dbv3* transcription, induced by adding thiostrepton, was 8 fold higher than in the wild type (Fig 34, see wt + tio and over *dbv3* + tio transcript levels).

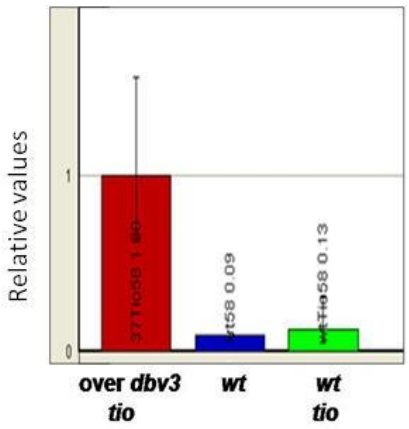

Fig. 34) qRT-PCR of *dbv3* transcript levels: in *Nonomuraea* wild type grown with thiostrepton (green) and without it (blue) and in the over *dbv3* mutant grown with thiostrepton (red).

Transcription level of one *dbv* gene per each poli-cistronic unit was analyzed. Two different qRT-PCR were performed: in the first *hrdb* was used as endogenous; in the second one 16s ribosomal RNA was used. All the analyzed genes are from 4 to 20 times more transcribed in over-*dbv3* mutant in respect to wild type in both analysis.

The first qRT-PCR analysis revealed that Dbv3 slightly influences *dbv1*, *dbv14*, *dbv28*, *dbv4* and *dbv6* and strongly controls *dbv15*, *dbv20*, *dbv26*, *dbv29*, *dbv36*, *dbv37* (Fig. 35).

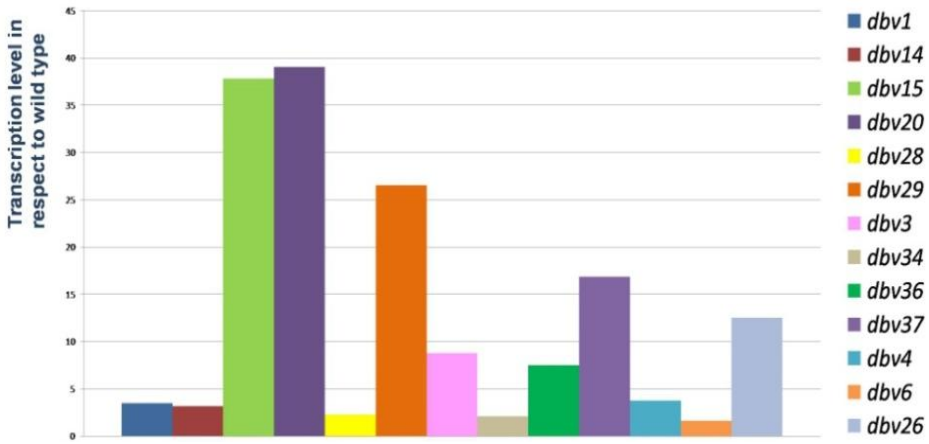

Fig. 35) qRT-PCR. Transcript levels of some *dbv* genes in over *dbv3* mutant in respect to *Nonomuraea* wild type; the values of wt were set equal to 1. *hrdb* was used as endogenous.

The second qRT-PCR analysis (Fig. 36) revealed that Dbv3 slightly influences *dbv15* and *dbv20* (4 fold more transcribed than in the wild type), and strongly controls *dbv14*, *dbv28*, *dbv34* (8 fold) and *dbv29* (18 fold).

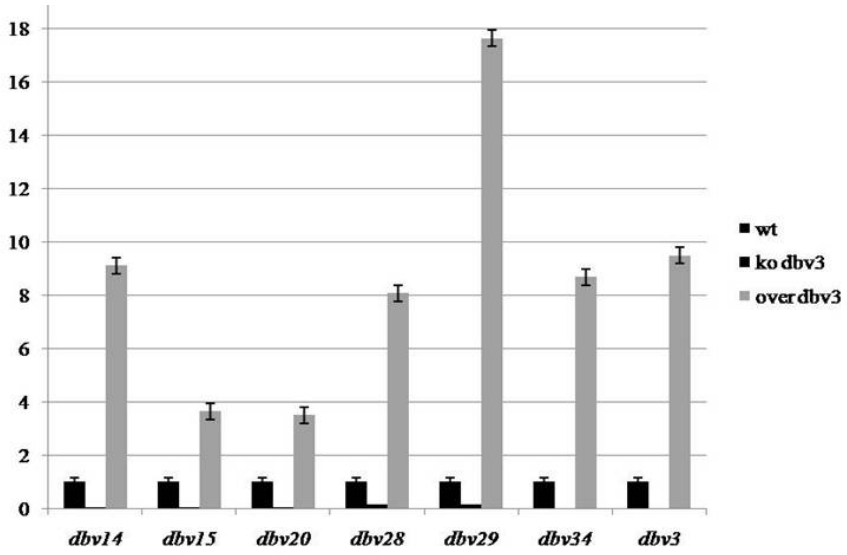

Fig. 36) qRT-PCR. Transcript levels of some *dbv* genes in over *dbv3* mutant in respect to *Nonomuraea* wild type; the values of wt were set equal 1). *16s* was used as endogenous.

Both analysis showed that *dbv3* is about 10 fold more transcribed in over *dbv3* mutant than in wild type and an increase in *dbv* transcript levels in the mutant. The differences between the two analysis consisted in the measurement of the increase of expression of individual genes: *dbv14* and *dbv34* are more transcribed in both real time analysis; according the first analysis 4 fold, according the second 9 fold more expressed than wild type.

In general, Dbv3 has a general positive role on most genes of the cluster. The *dbv6* and *dbv7* genes is not affected by *dbv3* over expression.

I**dentification of *dbv4* transcription start point**

The region upstream *dbv4* gene consists of 952 nucleotides. To determine the transcription start point (TSP) of the *dbv4* gene, RNAs were extracted after 24 and 48 hours of growth in Rare 3 medium and analyzed by S1 mapping experiment. Analysis demonstrated that *dbv4* transcriptional start site is around 330 nucleotides upstream the translational start site (Fig 37). The red arrow in figure indicates one of the two timidines that represent the transcription start site.

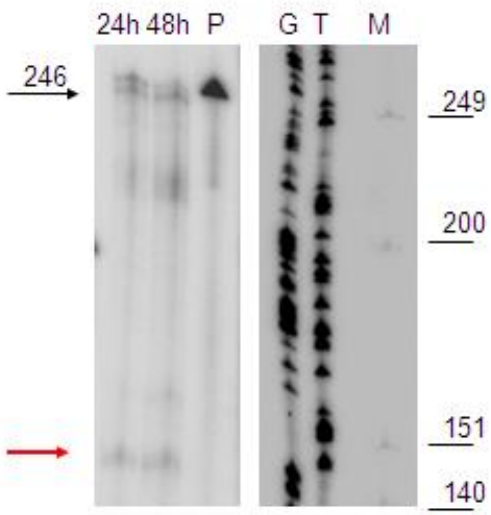

Fig. 37) Identification of *dbv4* transcription start point. 24 and 48 hours lanes represent the two samples; P:probe; M: marker; G and T represent the sequenced fragments

Identification of an IclR-like protein

Comparative analysis between the upstream region of *dbv4* and of the gene encoding the Str-like proteins in the *cep* gene cluster (that specify the biosynthesis of the glycopeptide antibiotics chloroeremomycin in *Amycolatopsis orientalis*) revealed the presence of a

common sequence of 43 nucleotides with 73% of identity (5'-cggagtgatcggaatgctaacgggaagcgttctgcaattcgat-3') named P4 (Fig. 38).

tcggtcttat ccgaaactag gggggtggat gtccgggata gggggtggtt cgacctgcac
agcctccttt aacc**tt**ccgg aggaaggcct aaccgaaagt **cggagtgatc ggaatgctaa**
cgggaagcgt tctgcaattc **gat**gaggtag acggctacgg attcgcggcg acagcgtcca
attctttgcc gcgtggagtt gccgaagaaa agaggatgcg acgcattctc tcgacagagc
acttggccga tcgatttatg cagctcgcgc cgggaagtcc aggcttgccc gggaccagat
gctgcaggcg cgacggggaa tcgtcgaagg tgcgcgcggc gcacgcggct gggttgtttt
ttgaacgccc ccggctccga tatgacgcta atcgaatcgg aggctag**gtg** gacccgacgg

Fig. 38) *dbv4* upstream region. It contains a conserved sequence of 43 nucleotides (underlined) named P4 localized 264 nucleotides upstream the translation start site (the gtg codone underlined). TT represent the TSP.

Conserved DNA regions among bacteria could have a functional meaning, *i. e.* a regulative role. The hypothesis is that this region could be a site of binding for positive or negative regulators of *dbv4* transcription and that this kind of mechanism of regulation is present in the *cep* cluster as well. So, in order to isolate protein/s binding to *dbv4* upstream region, P4 sequence was used as bait in a series of chromatographic steps.

Total proteins of *Nonomuraea* were extracted after 96 h of growth in RARE3 broth e EMSA were performed using P4 fragment as probe (Fig.39). Protein extracts bound P4, forming three different complex, indicated in figure as I, II and III complex (low, medium and high molecular weight, respectively). The signal of the complex I disappeared only when the concentration of cold P4 was 200X (data not shown); the signal of the complex II proportionally decreases with increasing specific competitor (lane 3 and 4); intensity of complex III remains unchanged with increasing competitor. The three complexes bind in a specific manner and with different binding affinities.

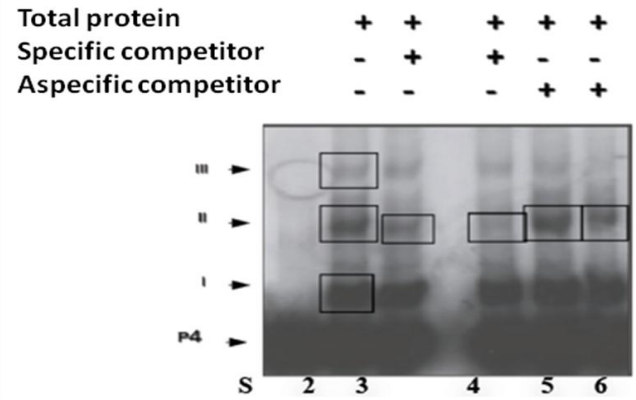

Fig 39) EMSA of P4 fragment with total protein extracts. I, II and III: low, medium and high molecular weight complex respectively

To isolate the proteins of *Nonomuraea* that bind specifically the P4 fragment, total protein extract was fractionated by precipitation with increasing amounts of ammonium sulphate concentrations and were subdivided into the three fractions 0-30%, 30-60% and 60-100%. The three fractions were used to test binding to the P4 probe in EMSA (Fig 40).

The analysis showed the formation of different kinds of shift for the fractions 30-60 % (complexes II and III, lane 2) and 60-100% (complex I, lane 1).

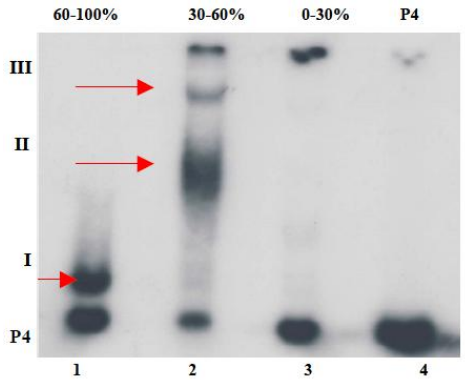

Fig.40) EMSA of P4 with the three protein fractions 0-30%, 30-60% and 60-100% fractionated by precipitation with ammonium sulphate. I, II and III: low, medium and high molecular weight complex respectively

The samples of the fractions 30-60% and 60-100% were subjected to dialysis and fractionated by cation exchange chromatography using FPLC system with columns Mono S PC 1.6/5^{TM} (Amersham© Pharmacia Biotech).

For the 60-100% fraction, elution of the proteins bound to the column were performed (Fig. 41) using five growing concentrations of NaCl: 25% (NaCl 0,25 M), 50% (NaCl 0,5 M); 75% (NaCl 0,75 M); 100% (NaCl 1 M); 200% (NaCl 2 M).

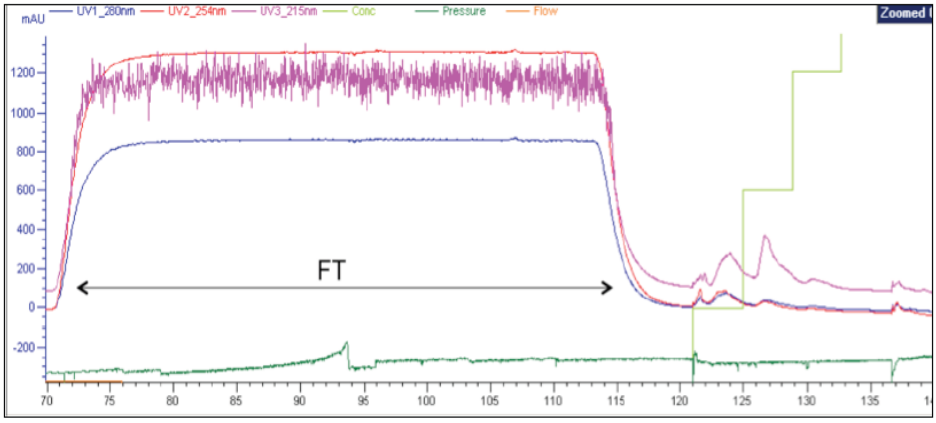

Fig. 41) Cation exchange chromatography of the 60-100% fraction after precipitation with ammonium sulphate. Blue line: the signal from the proteins that absorb in 280 nm, pink line: signal from the proteins that absorb at 215 nm, red line: the signal from proteins that absorb at 254 nm; dark green line: pressure; light green line: discontinuous elution of NaCl (step I = 0.25M; step II = 0.50M; step III = 0.75M; step IV = 1 M).

The five fractions were subjected to dialysis and used to test binding to the P4 probe in EMSA (Fig.42). All the fractions, except flow trough and protein fraction 25% NaCl (lane 4 and 5), gave at least one shift.

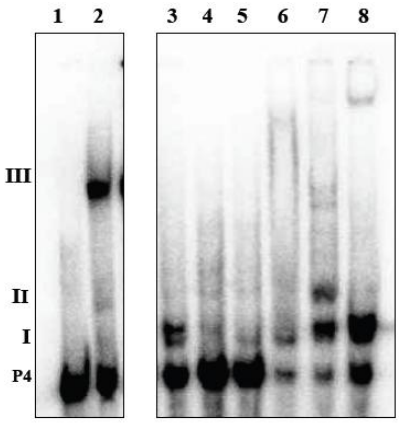

Fig. 42) EMSA of P4 with the five fractions obtained by cation exchange chromatography of the 60-100% fraction (obtained by precipitation with ammonium sulphate). I, II and III: low, medium and high molecular weight complex respectively. lane1 probe (P4); lane2, crude extract; lane3, 60-100% fraction before chromatography; lane4, flow trough; lane5, fraction 25% NaCl; lane6, fraction of 50% NaCl; lane7, fraction 75% NaCl; lane8, 100% NaCl fraction.

The specificity of binding to P4 of the fractions 75%, 100% and 200% NaCl was tested using the specific competitor (cold P4). This analysis revealed that the binding was specific because the shift signal decreased after addition of the specific competitor (Fig. 43).

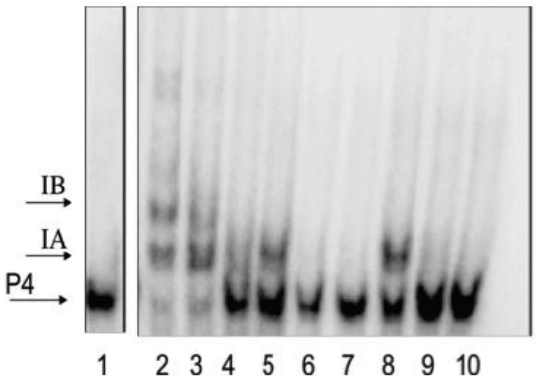

Fig 43) EMSA of P4 with the 75%, 100% and 200% NaCl fractions obtained by cation exchange chromatography of the 60-100% fraction (obtained by precipitation with ammonium sulphate). lane1: probe (P4); lane2: 75% fraction; lane3: fraction 75% in presence of 50X specific competitor (P4); lane4: 75% fraction in presence of 200X specific competitor; lane 5: fraction 100%; lane 6: 100% fraction in presence of 50X specific competitor; lane 7: 100% fraction in presence of 200X specific competitor; lane 8: 200% fraction; lane 9: 200% fraction in presence of 50X specific competitor; lane 10: 200% fraction in presence of 200X specific competitor. I, II and III: low, medium and high molecular weight complex respectively.

The fractions 75%, 100% and 200% have been joined and fractioned into 15 samples by cation exchange chromatography with increasing concentration of NaCl (from 50 mM to 2 M, Fig. 44).

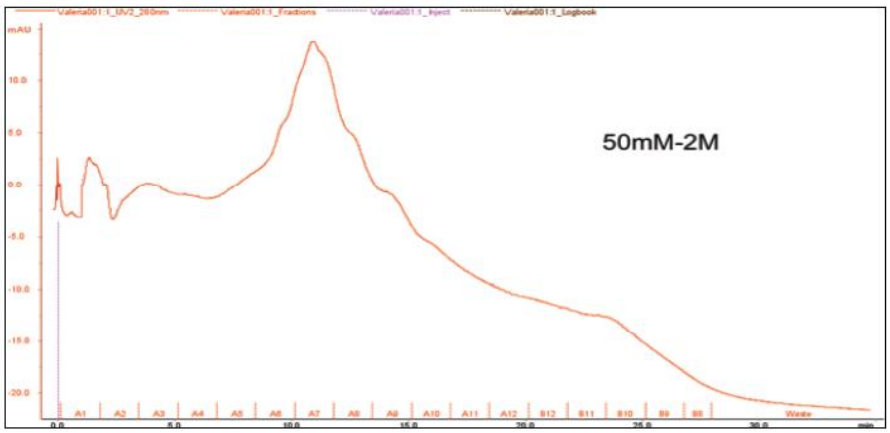

Fig. 44) Cation exchange chromatography with increasing concentration of NaCl (from 50 mM to 2 M) of the fractions 75%, 100% and 200% have been united into one. red line: the signal from proteins that absorb at 80 nm.

All the fifteen fractions were used to test binding to the P4 probe in EMSA (Fig.45). Only three fractions (samples 6, 7 and 8) gave the low molecular weight shift (complex I).

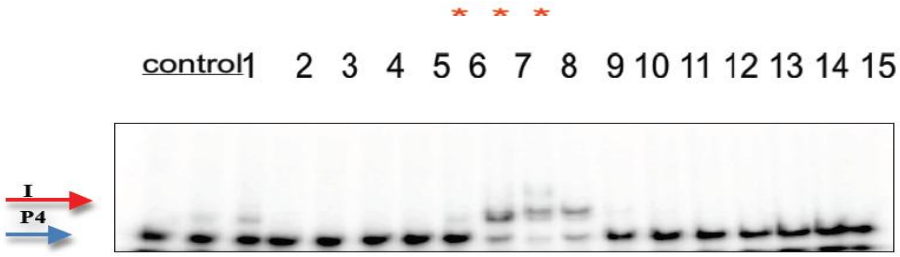

Fig. 45) EMSA of P4 fragment with the 15 protein fractions eluited after Cation exchange chromatography with increasing concentration of NaCl. I: low molecular weight complex. The asterisks indicate the fractions that gave shift.

The three fractions have been joined and further fractioned into 17 samples by anion exchange chromatography (Fig. 46) using columns Mono Q PC 1.6/5^{TM} (Amersham© Pharmacia Biotech).

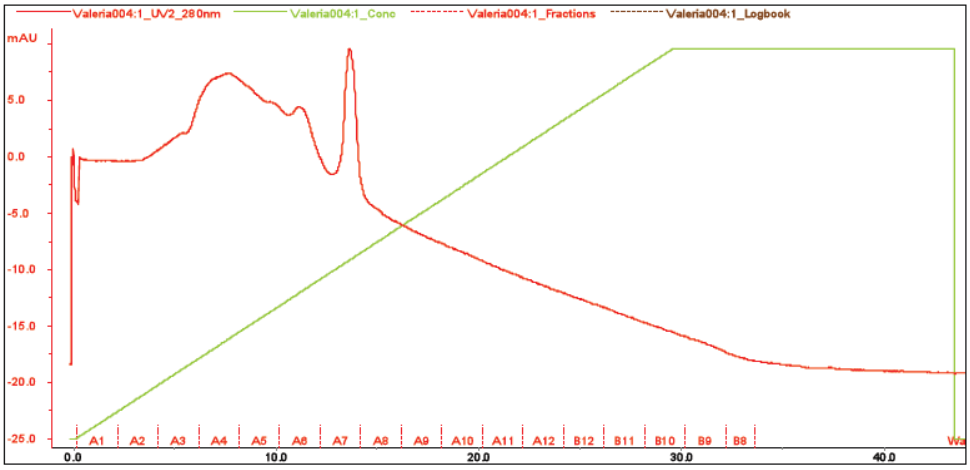

Fig.46) Anion exchange chromatography using columns Mono Q PC 1.6/5^{TM} of the samples 6, 7, 8 obtained with Cation exchange chromatography. red line: the signal from proteins that absorb at 280 nm; light green line: continuous elution of NaCl.

All the fourteen fractions were used to test binding to the P4 probe in EMSA (Fig.47). Only one fraction (sample 4, named X1) gave the low molecular weight shift (complex I).

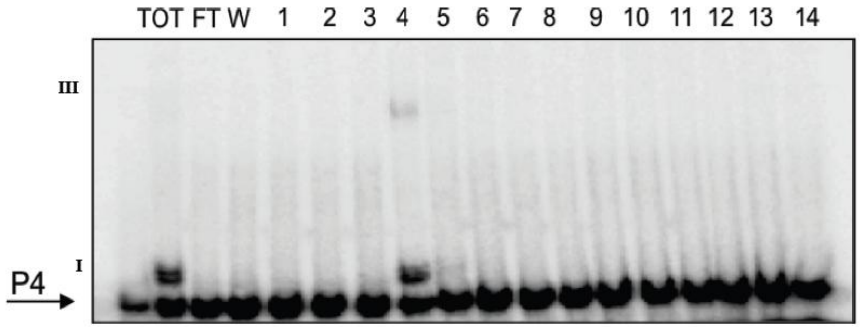

Fig. 47) EMSA of P4 fragment the 14 fractions obtained after elution of anion exchange chromatography. I and III: low and high molecular weight complex. Tot: total protein from *Nonomuraea*; FT: flowthrought; W: probe.

In parallel, the 30-60% fraction (obtained by precipitation with increasing amounts of ammonium sulphate) was fractionated by cation exchange chromatography. Elution of the proteins bound to the column was performed using growing concentrations of NaCl (Fig 48).

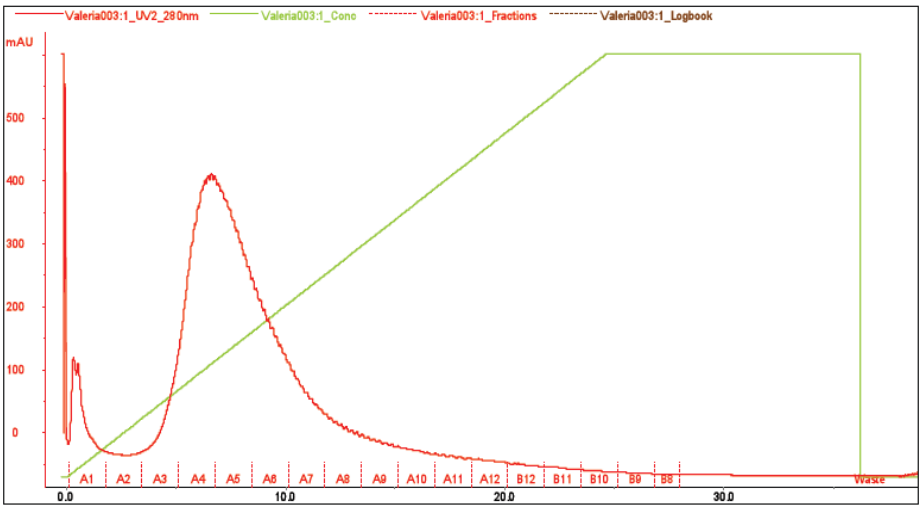

Fig. 48) Cation exchange chromatography of the 30-60% fraction (obtained by precipitation with increasing amounts of ammonium sulphate). red line: the signal from proteins that absorb at 280 nm; light green line: continuous elution of NaCl.

17 fractions were collected and 12 of these were used to test binding to the P4 probe in EMSA (Fig.49). Samples 4 and 5 gave a shift of high molecular weight. Sample 6 and 7 gave a shift of lower molecular weight.

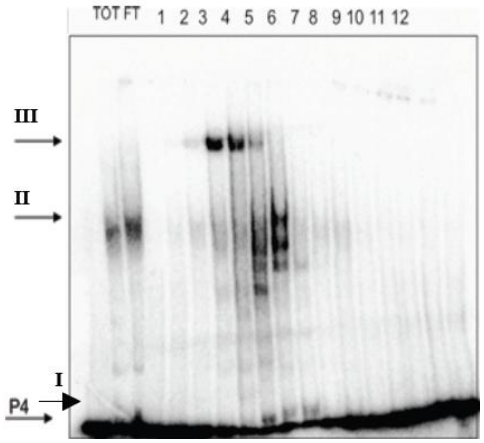

Fig.49) EMSA of P4 fragment with 12 fractions obtained after elution of cation exchange chromatography. I, II and III: low, medium and high molecular weight complex. Tot: total protein from *Nonomuraea*; FT: flowthrought.

Protein samples X1 (lane 4, Fig. 47), X2 (lane 4 and 5, fig.49) and X3 (lane 6 and 7, fig.49) were then subjected to affinity chromatography by using metal micro-beads (MagneSphere Magnetic® by Promega© P4) streptavidin-coated, linked to the biotinylated P4 (pull down experiment). After chromatography, the three eluted samples were used to test binding to the P4 probe in EMSA (Fig.50). In this ionic condition, all the three samples gave the same shift. For each sample, a negative control with beads and total proteins was carried out.

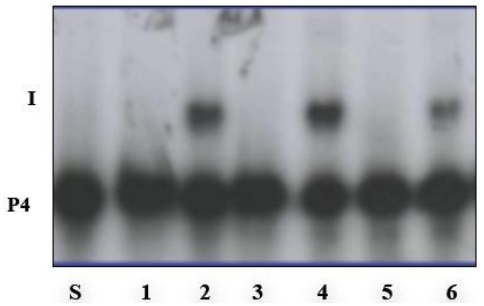

Fig.50) EMSA of P4 the samples X1, X2 and X3 subjected to affinity chromatography by using metal micro-beads. I: low molecular weight complex. S:probe P4; lane 1: MagneSphere® and proteins X1; lane 2: MagneSphere®P4 and proteins X1; lane 3: MagneSphere® and proteins X2; lane 4: MagneSphere®P4 and proteins X2; lane 5: MagneSphere® and proteins X3; lane 6: MagneSphere®P4 and proteins X3.

Eluited samples were loaded into a 12% SDS PAGE gel; the gel was silver stained (Fig. 51) and spots of the single proteins (indicated with a number) were characterized by mass spectrometry (LC/MS-MS analysis). In this way the following proteins were identified:

- Spot 1: guanosine pentaphosphate synthetase I/polynucleotide phosphorylase
- Spot 4: ribonuclease, Rne/Rng family
- Spot 13: tRNA (adenine-58-N(1)-) methyltransferase
- Spot 14: transcriptional regulator of the IclR family

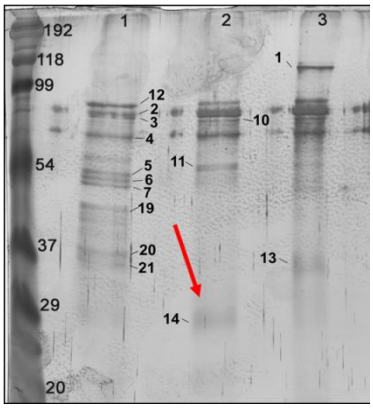

Fig. 51) SDS PAGE of protein fractions isolated by different chromatographic steps. The spot number 14, indicated by the red arrow corresponds to an IclR-like protein.

Some of them, like 1, were present in only a sample; others, like 4 and 14, could be present in all the three samples. Among the identified proteins, the regulator IclR was the most interesting. Thus, qRT-PCR was performed, using RNA extracted from *Nonomuraea* wild type cultivated in a defined growth medium containing either 4.2 or 2 mM phosphate (HighP and LowP conditions, respectively). As shown in fig. 9, after 35 h of growth A40926 production started in both media, but after 47 h the A40926 yield was different in the two phosphate conditions: A40926 was produced in higher amount in LowP condition in respect to HighP condition.

The qRT-PCR analysis showed that the levels of transcription of genes *iclR* and *dbv4* have an opposite trend: *iclR* was more transcribed when a low yield of antibiotic was produced (high phosphate, Fig. 52); *dbv4*, viceversa, was more transcribed when antibiotic production was higher (low phosphate, Fig. 52).

These preliminary data suggested a possible negative involvement of IclR in A40926 production. Since the DNA fragment used as bait in pull-down experiments is localized downstream the transcriptional start site, a negative role of IclR in *dbv4* transcription is likely to occur.

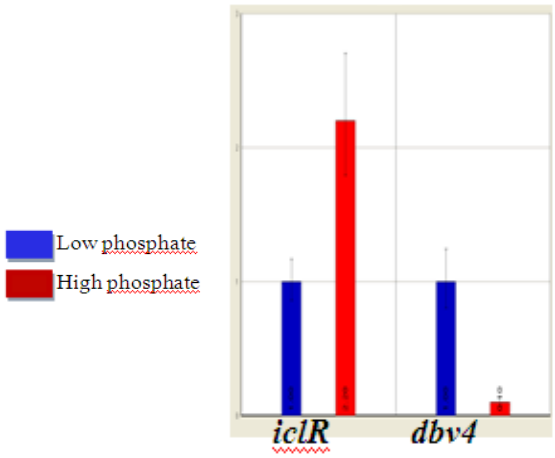

Fig. 52) qRT-PCR of *iclR* e *dbv4* *Nonomuraea* wild type grown on broths called highP e lowP.

Generation of putative knock out mutant

To further characterize *iclR*, a strategy to generate an *iclR* mutant (Ko *iclR*), by using the pIJ773 plasmid, a suicide vector for *Nonomuraea*, was carried out. An internal fragment of the *iclR* gene was cloned into the plasmid. The integration of the plasmid by single crossing over should had led to the interruption of the gene *iclR*.

After many attempts, due to the fact that genetic manipulation in this strain is not efficient, three putative Ko *iclR* clones resistant to apramycin were obtained, named heart, star and sun.

Effect of *iclR* inactivation in three putative knock out mutants

All the three putative Ko *iclR* mutants showed some features very different from *Nonomuraea* wild type. On solid V0.1 the mutants grew slowly and lacked of the typical pigmentation of *Nonomuraea*, remaining white even in the late stages of growth.

Disruption of the *iclR* gene did not significantly alter growth kinetics in the rich broth R3 during the first 140 hours of growth (Fig. 53). The differences in growth rate became significant later in the growth.

As negative regulator, we expected to obtain a knock out mutant that produced higher amount of antibiotic. Surprisingly, microbiological assays showed that the putative mutants produced very late (after 164 hours), while *Nonomuraea* wild type activated antibiotic production at 70 hours. To explain this result we suggested that other pathways could be affected by IclR.

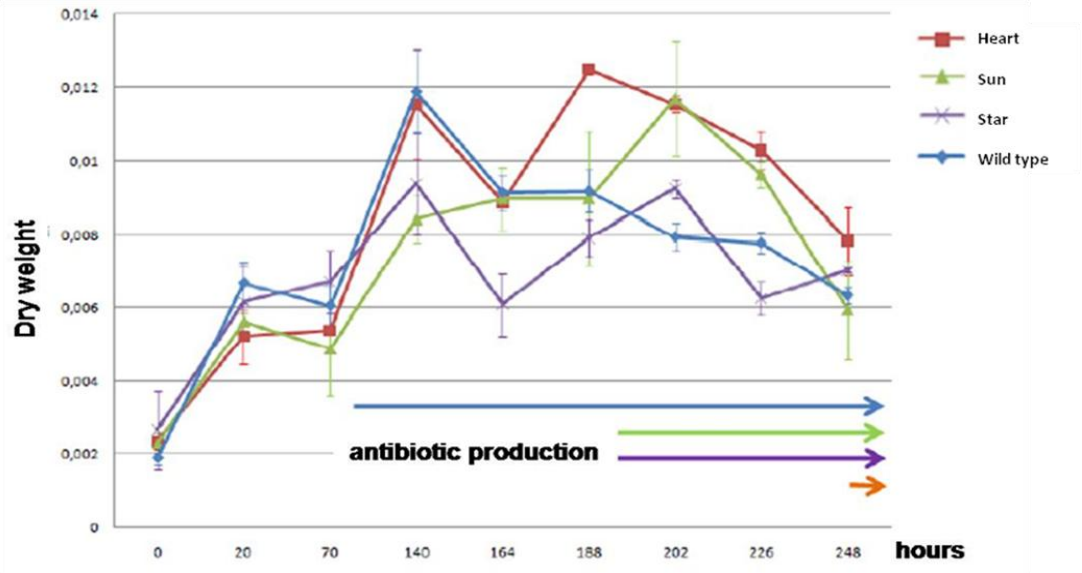

Fig. 53 Growth of the three putative Ko *iclR* mutants and *Nonomuraea* w. t. in R3.

Since IclR was found to be involved in glyoxylate shunt or growth on citrate as carbon source, a biochemical characterization of *Nonomuraea* was carried out.

Firstly, the glucose concentration in the culture medium was measured at different times of growth revealing a different pattern of glucose concentration between the putative Ko *iclR* mutants and the wild type: in fact in the early stages of growth, glucose was not consumed by the Knock out mutants, but increased with a peak around 20 hours (Fig.54). After 70 hours of growth a drastic reduction of glucose was observed in both wild type and star and sun mutants; already at 140 hours of growth the concentration of glucose was no longer detectable by the instrument used in the laboratory.

These results suggested that the putative mutants exhibit an alteration in glucose metabolism; in particular it would seem that in the early stages of growth the mutants strangely do not activate the glucose catabolism, but instead they do gluconeogenesis.

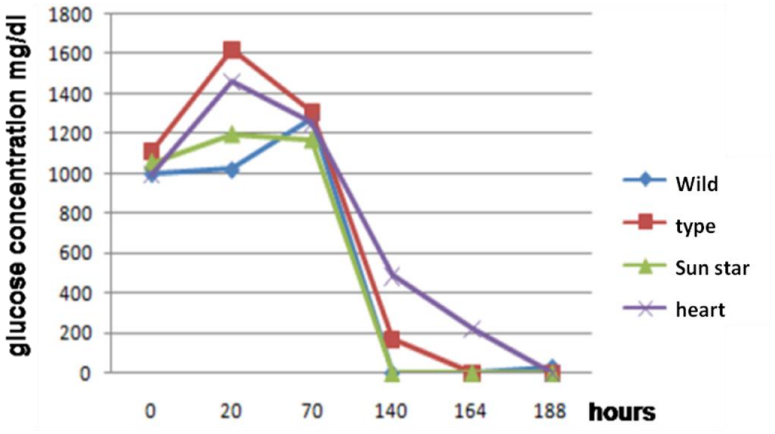

Fig. 54 Glucose concentration during growth of the three Ko *iclR* mutants.

On solid V0.1, a poor medium, the mutants grew very slowly. To investigate the metabolic pathways which had been altered in the mutant strains, several feeding experiments were conducted.

The addition of leucine, cysteine, methionine and casaminoacids to the minimal medium was not sufficient to restore growth and pigmentation in the Ko *iclR* mutants.

This suggested that IclR controls other metabolic pathways in *Nonomuraea*.

Different carbon sources and intermediates of the Krebs cycle were added to the minimal medium in order to restore growth kinetic and/or pigmentation (table 2).

The wild type strain was capable to grow in presence of glucose as sole carbon source, and in presence of both glucose and glycerol or glucose and acetate. In contrast, in presence of glycerol as sole carbon source, *Nonomuraea* wild type grows slower, and in presence of acetate as sole carbon source, it does not grow, suggesting that *Nonomuraea* prefers to use glucose as carbon source.

In presence of glucose, mutants showed a slower growth compared to the wild type strain. The addition of yeast extract, which is a complex mixture of carbon sources, allowed the growth of the mutants with a growth kinetics comparable to wild type. The acetate is not

used by all the strains and does not allow growth even in the presence of glucose. In the presence of glycerol the wild type strain grows slowly; mutants, however, do not grow even when glucose is added to the medium.

	Wt	HEART	SUN	STAR
YE+Glu	+	+	+	+
YE	+	+	+	+
Glu	+	CR	CR	CR
Gly	CR	-	-	-
Ace	-	-	-	-
Cit	-	-	-	-
Glu+Gly	+	-	-	-
Glu+Ace	+	CR	CR	CR
Glu+Cit	-	-	-	-
Glu+Ace+Cit	-	-	-	-

Table 2 Growth of wild type and ko iclR mutants in Minimal Medium containing different carbon sources: Glu: glucose, YE: yeast extract, Gly: glycerol; Ace: acetate; CiT: citrate +: growth - growth failure, CR: slow growth.

This suggested that the mutant strains are unable to metabolize glycerol and that the presence of glycerol alters uptake and/or metabolism of glucose.

None of the compounds used restores pigmentation in mutant strains.

Construction of *iclR* over expression mutant

Five mutants of over-expression of the gene *iclR* (over *iclR*) were generated. pIJ8600, an integrative plasmid for Actinomycetes, was used to add a copy of the *iclR* gene in the *attB* site of bacterial chromosome. The genomic integration of pIJ8600-*iclR* in the mutant was verified by PCR (Fig. 55) and Southern blot analysis (Fig. 56).

For the PCR analysis, primers that bind on the two sides of the cloning site of the pIJ8600 plasmid were used. If pIJ8600 was integrated into *Nonomuraea* chromosome, a PCR product of 700 bp (that is the length of the *iclR* gene inserted) is expected. In the picture 55, clones 8, 10, 28, 14, 29, 34 and 33 gave the corret size PCR product (indicated by grey arrows).

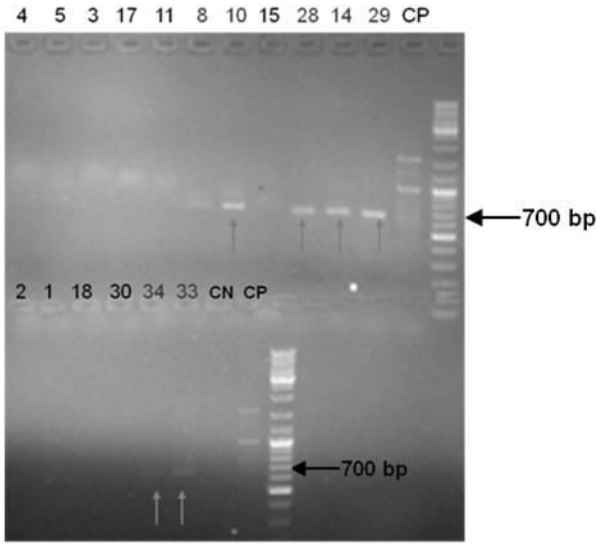

Fig.55 PCR of *over iclR* mutants. Genomic DNAs from Clones 8, 10, 14, 28, 29, 33 and 34 gave the 700 bp PCR product. CP: empty pIJ8600; CN: *Nonomuraea* wild type.

A Southern blot analysis was performed using as probe pIJ8600-*iclR* digested with *PstI* (fig. 56), a signal at 1,1 kb was detected both in the wild type (lane 3) and in the over *iclR* mutant clone 14 (lanes 4), indicating the hybridization of the wild type copy of *iclR* gene

with the probe. Moreover, another signal is present for the mutants, bigger than 3 kb, corresponding to the additional copy of *iclR*.

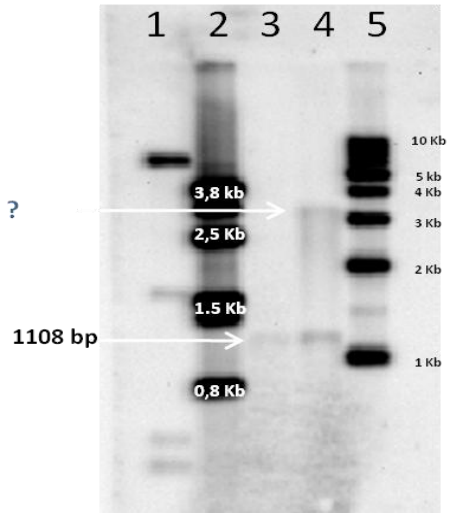

Fig 56) **Southern blot analysis of over *iclR* mutant 14i** (lanes 4) and *Nonomuraea* wild type (lane3) DNA digested with *Pst*I, using as probe pIJ8600-iclR digested with *PstI* (lane 2).

Effect of *iclR* over-expression

The five over *iclR* mutants (8i, 10i, 14i, 29i, 37i) showed morphology, pigmentation and growth rates similar to *Nonomuraea* wild type on R3 agar plates, while in liquid R3 over *iclR* mutants showed a higher rate of growth and a more intense pigmentation than *Nonomuraea* wild type. The microbiological assays revealed that *Nonomuraea* wild type produced A40926 from 72 hours and that none of the putative over-expression mutants produced the antibiotic. The absence of antibiotic production in the putative mutants suggested that IclR has a negative role in A40926 biosynthesis, and a positive effect on

growth; in fact all the mutants accumulated a larger amount of biomass in respect to wild type (Fig.57).

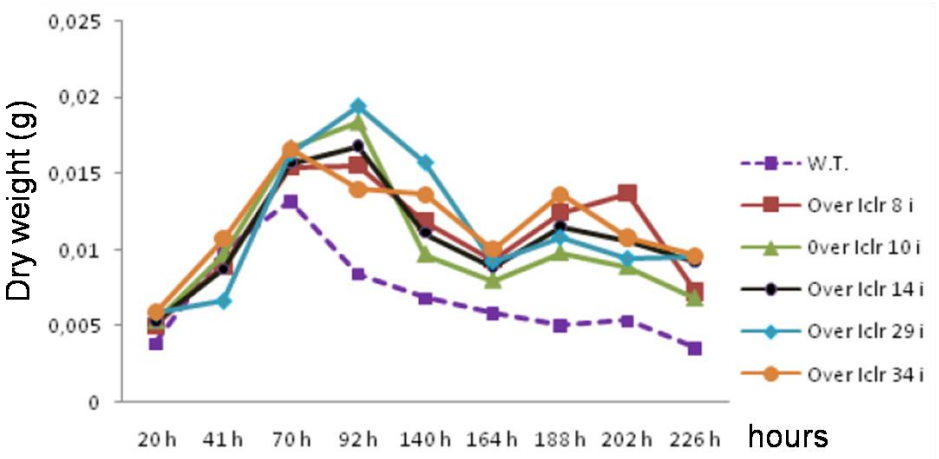

Fig. 57 Growth of *Nonomuraea* wt and the five over *iclR* mutants in R3

In vitro binding of His6-tagged IclR

To investigate the activity of IclR, an His6-tagged IclR was prepared. The pRSETB, an expression plasmid, was used to insert the *iclR* gene downstream and in frame with a sequence coding for six histidines. The promoter that controls the transcription of the gene of interest is the strong promoter for phage T7 DNA polimerase. The construct was inserted into the cells of *E. coli* BL21 AI, in which the transcription of the T7 polymerase is inducible by arabinose. The BL21Ai pRSETB-IclR clone was induced with 0,2% of arabinose for two hours, when BL21 AI cells at 37 °C reached an $O.D_{600}$0,6. The His tagged IclR protein was purified using Ni-NTA Purification System (Invitrogen). Western blotting analysis, using Anti-His G-AP Antibody (invitrogen), confirmed the presence of the protein sample eluited with 200mM imidazole (Fig. 58).

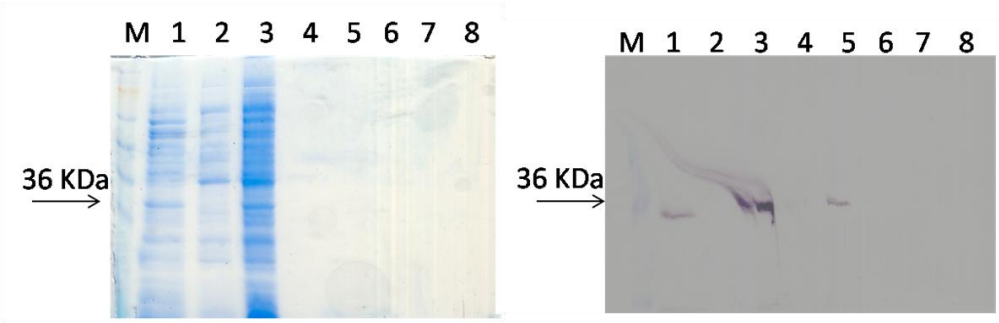

Fig. 58) SDS page (left) and Western blot analysis (right) of M: Marker, See pre-stained standard (Invitrogen); 1: flowthrought; 2: wash1; 3: total proteins; 4: proteins eluted with 100 mM imidazole; 5: proteins eluted with 200 mM imidazole; 6: proteins eluted with 300 mM imidazole; 7: proteins eluted with 400 mM imidazole; 8: proteins eluted with 500 mM imidazole.

Gel mobility shift assays (EMSA) were carried out using the purified His6-tagged IclR. Different DNA probes were prepared. Three probes were obtained by PCR: one contains the entire upstream region of *dbv4* gene and two contain about half part of the entire region and overlap. P4 was prepared by annealing of two oligonucleotides.

All these probes were used in EMSA experiments with His6-tagged IclR but no bindings were detected.

Discussion

The attinomicete *Nonomuraea* sp. ATCC 39727, genetically and physiologically poorly characterized, is known for its ability to produce the antibiotic A40926. The study of the morphology and physiology of *Nonomuraea* can broaden the knowledge of the mechanisms of regulation of gene expression and could lead to the understanding of the relationships between primary and secondary metabolism. In addition, new knowledge would enable the rational handling of *Nonomuraea* in order to increase production yield of the antibiotic A40926.

In particular, the present study was aimed to elucidate A40926 biosynthesis regulation in *Nonomuraea sp.* ATCC 39727. Thus, we examined the functions of the transcriptional regulatory genes, *dbv3*, *dbv4*, *dbv6* and *dbv22* that lie in the A40926 gene cluster in *Nonomuraea* and *iclR*, whose gene is outside the *dbv* cluster.

Dbv3 and Dbv4

Our experiments demonstrated, for the first time, that the transcription activator genes *dbv3* and *dbv4* are both required for A40926 biosynthesis. In fact, both Ko *dbv3* and Ko *dbv4* mutants have completely lost the ability to produce A40926.

This study confirmed the function of Dbv4 as a positive regulator of A40926 biosynthesis by activating expression of two operons of the *dbv* cluster: the *dbv14-dbv8* operon, encoding the four cross-linking oxygenases, the halogenase, the N-acetylglucosamine transferase and the N-acylase, and the *dbv30-dbv35* operon, encoding the four enzymes involved in DPG biosynthesis (Chen *et al.,* 2001; Pfeifer *et al.*, 2001), as well as the sodium proton antiporter and a protein of unknown function. Indeed, RT-PCR analysis demonstrated that *dbv14-dbv8* and *dbv30-dbv35* operons are not transcribed in Ko *dbv4*

mutant (Fig.27), confirming that Dbv4 is the pathway-specific regulator in A40926 in biosynthesis.

All the five other gene clusters devoted to glycopeptides (chloroeremomycin, balhimycin, complestatin, A47934, and teicoplanin) contain an *strR*-like regulator (Donadio *et al.*, 2005). In vitro Dbv4 is able to bind to two palindrome sequence GTCCA $(N)_{17}$TTGGAC, upstream to *dbv14* and *dbv30* genes while it was clearly unable to bind to its own upstream region (Alduina *et al.*, 2007). The *bal* cluster encodes a Dbv4 ortholog, named Bbr, which specifically binds to the upstream regions of five *bal* genes, including itself (Shawky *et al*., 2007) such as StrR controls its own expression (Retzlaff *et al.*, 1995) and probably the same occurs in the chloroeremomycin case because in silico analysis indicate the presence of StrR binding site upstream the StrR-like gene (Fig. 11, "c" light blue circle). Similarly to Dbv4, the StrR-like regulator is not expected to control its own expression in the *sta* and *tcp* clusters (the upstream regions of StrR- like genes lack of StrR binding site; Fig. 11, "c" light blue circle).

Dbv4 and Bbr, which share 80% identity, possess the same predicted helix-turn-helix motif and very similar dimerization domains. Moreover, Bbr is able to bind *dbv* sequences and, vice versa, that Dbv4 recognizes at least some *bal* sequences (Alduina *et al.*, 2007).

The *dbv* cluster appears to contain just two binding sites for Dbv4 while the *bal* cluster contains five Bbr binding sites (Shawky *et al.*, 2007) and the *cep, sta,* and *tcp* clusters should contain at least two, one, and four predicted Dbv4-binding palindromes, respectively (Donadio *et al.*, 2005). In all five clusters, one putative binding site is located 5' to *oxyA* orthologs. This gene encodes the P450 mono-oxygenase responsible for cross-linking amino acids 2 and 4 (Bischoff *et al.*, 2005). The Oxy enzymes catalyze a critical step, probably the most distinctive feature in glycopeptide biosynthesis. Since all glycopeptide clusters encode an StrR-like regulator, it is tempting to speculate that expression of the oxy genes is controlled in all clusters by the same regulator.

To understand the hierarchy between *dbv3* and *dbv4*, RT-PCR analysis of *dbv3* revealed that *dbv3* is transcribed in Ko*dbv4* mutant, demonstrating that Dbv4 does not control *dbv3* transcription (Fig. 27).

Computer-assisted analysis of the Dbv3 protein revealed that it belongs to LAL (large ATP-binding regulators of the LuxR family) family. Dbv3 protein possesses typical LuxR family characteristics, including an ATP/GTP-binding domain at the N-terminal and a DNA binding helix-turn-helix domain at the C-terminal. The Walker A and B motifs are characteristic of a large family of ATPases that have been associated with diverse cellular activities, including cell cycle regulation, protein degradation and protein transport. The presence of ATP/GTP binding Walker A and B motifs suggests that their activity is dependent on ATP/GTP hydrolysis.

We found that in the Ko *dbv3* mutant *dbv4* gene is not transcribed (Fig. 28). Moreover, qRT-PCR of some *dbv* genes revealed that in Ko *dbv3* mutant transcript levels of *dbv* genes are six - ten fold lower than in wild type (Fig. 29). According to the data presented here, we can suggest that Dbv3 is a transcription regulator that hierarchically acts before Dbv4, exerting its control also over the *dbv* genes.

Several regulators of the LAL family have been identified in antibiotic and other secondary metabolite gene clusters from actinomycetes, including PikD from the pikromycin pathway in *S. venezuelae* (Wilson *et al.*, 2001), RapH from the rapamycin pathway in *S. hygroscopicus* (Aparicio *et al.*,1996; Kuščer et al. 2007), NysRI and NysRIII from the nystatin pathway in *S. noursei* (Sekurova *et al.,* 2004), and AmphRI and AmphRIII from the amphotericin pathway in *S. nodosus* (Carmody *et al.*,2004; Caffrey *et al.,* 2008), SsaA from the sansanmycin pathway in *Streptomyces sp* (Li *et al.,* 2013), SanG from nikkomycin pathway in *Streptomyces ansochromogenes* (He *et al.,* 2008), FkbN from

FK506 pathway in *Streptomyces tsukubaensis* (Goranovĭc *et al.,* 2012). All these examples of LAL proteins have are regulator with a positive role in antibiotic production.

Instead, JadR, a γ-butyrolactone receptor homologue (Wang and Vining, 2003), is a repressor gene that negatively regulates jadomycin production in *S. venezuelae* ISP5230. Its disruption led to jadomycin production without environmental stress and increased production level when stressed (Yang *et al.,* 1995).

In this work we demonstrated that Dbv3 is a positive regulator of A40926 production. In fact, disruption of *dbv3* gene led to loss of antibiotic production; in Ko *dbv3* mutant the positive regulator *dbv4* is not transcribed as well as various genes in the cluster (Fig. 28 and 29).

Two LAL regulators in *S. coelicolor* have recently been identified that control the biosynthesis of the blue pigmented antibiotic actinorhodin but also act globally affecting various cellular processes, and amongst them the phosphate starvation response (Susana *et al.,* 2012). So a pleiotropic role has been recognized to LAL proteins in actinomycetes.

Disruption of *dbv3* did not significantly alter kinetic growth. In fact, the mutants showed the same growth rate and morphological characteristics as the parent strain on several media (i.e. R3, MS, V01 solid media, or R3 liquid medium) indicating that the *dbv3g*ene is not critical for bacterial growth and differentiation. These results suggest that Dbv3 is a pathway-specific regulator.

Dbv3 could be a target to increase antibiotic yield. To generate a strains that overproduces A40926, a *dbv3* over expression mutant was generated, capable to produces earlier and more antibiotic than wild type (Fig. 33). So, the impact of overexpression of *dbv3* on A40926 production confirmed that it is a positive regulator. Interestingly, other *dbv* genes were more transcribed than in the wild type (Fig. 35 and 36).

The absence of homology between the upstream regions of all the *dbv* genes whose transcript levels are higher after *dbv3* over-expression, suggests that the *dbv3* control on the cluster could be indirect. Further functional studies of Dbv3 may help to better elucidate the regulation of glycopeptide production.

dbv3 and *dbv4* contain one and three TTA codons, respectively, so their expression might be dependent also on *bldA*, the structural gene for tRNA UUA, if this mechanism operates in *Nonomuraea* as well.

IclR

In experiments of affinity chromatography using as bait a DNA fragment upstream of the gene *dbv4* (called P4) and then elettroforetic mobility shift assay (EMSA), a protein IclR-like has been identified (Fig. 51).

IclR family comprises regulators acting as repressors, activators and proteins with a dual role (activator and repressor). Members of the IclR family control genes whose products are involved in the glyoxylate shunt (Sunnarborg *et al.*, 1990), multidrug resistance (Beinlich *et al.*, 2001; Grkovic *et al.*, 2001; Guazzaroni *et al.*, 2005), degradation of aromatics (Tsoi *et al.*,1999; Romero-Steiner *et al.*,1994), inactivation of quorum-sensing signals (Zhang *et al.*, 2004), antibiotic production (Santamarta *et al.*, 2007; Kim *et al.*, 2012) and sporulation (Jiang & Kendrick, 2000; Yamazaki *et al.*, 2003; Zhu & Winans, 1999).

Since P4 is localized downstream *dbv4* transcription start site (Fig. 38, mapped by S1-mapping experiments, a negative role to IclR was hypothesized. Indeed, qRT-PCR analysis showed that the levels of transcription of genes *iclR* and *dbv4* have an opposite trend: *iclR* is more transcribed when a low yield of antibiotic is produced; *dbv4*, vice versa, is more transcribed when antibiotic production is high (Fig. 52). These preliminary data suggested a possible involvement of IclR in A40926 production.

The morphological and physiological analysis of ko *icl*R putative mutants reveals that they do not grow in minimal medium solid and lack of pigmentation in all the used media. The analysis of the growth in rich medium (Fig. 53) shows that the non-pigmentation may not be related to a slowdown in the growth stages, but to metabolic abnormalities that need to be investigated.

It is well known that IclR-like proteins are involved in the ability of bacteria to grow in certain soils. For example in *S. clavuligerus* AreB, which gene is located upstream and in opposite orientation to the *leuCD* operon, controls biosynthesis of leucine and of the two antibiotics clavulanic acid and cephamycin C (Santamarta *et al*., 2007). The growth of the *areB* mutant is restored by the addition of leucine to the minimal medium. In *S. coelicolor* Knock out mutant in *ndgR*, which encodes a IclR-like protein and which is also located upstream and in opposite orientation to the *leuCD* operon, grows in minimal medium only after the addition of cysteine and methionine.

Also in *Nonomuraea iclR* gene is located upstream and in opposite orientation to the *leuCD* operon (Alifano, unpublished data).

In order to delineate the metabolic pathways controlled by *iclR* in *Nonomuraea*, different carbon sources and different amino acids were added to the minimal medium. None of the amino acids was sufficient to restore growth and pigmentation in Ko mutants. Further feeding experiment are necessary to establish what metabolic pathway was altered in Ko *iclR* mutants.

IclR seems to be involved in the metabolism of the carbon sources. In fact, the mutant strains are unable to metabolize glycerol; interestingly, glycerol seems to alter the uptake and /or metabolism of glucose (Table 2). To my knowledge, to date has not yet been clarified what carbon sources is preferentially used by *Nonomuraea* and carbon catabolite repression mechanisms have not yet been identified. Here a new model has been suggested according to which in the presence of glycerol IclR may act as an activator of the glycerol

catabolism. Glycerol also seems to suppress the catabolic pathway of glucose. According to this model the glycerol is chosen from *Nonomuraea* as a favorite carbon source.

To confirm this hypothesis glucose consumption could be measured during growth in liquid minimal medium, in the presence of glycerol or glucose.

Dbv6 and Dbv22

Microbiological assays suggest that *dbv6* could be positively involved in the regulation of resistance to the glycopeptides. Dbv6 is a protein VanR-like while Dbv22 could be the sensor on the membrane. VanS and VanR are an example of a two-component system, identified in pathogenic bacteria resistant to the glycopeptide vancomycin (Hong *et al*, 2008). In *S. coelicolor* it has been shown that VanS and VanR activate the transcription of *vanHAX* genes, for resistance to the glycopeptide antibiotic vancomycin.

In *Nonomuraea* Dbv6 could regulate *vanY* gene transcription, whose product is involved in the mechanism of self-resistance. VanY (196 residues) is encoded by the *dbv7* gene within the *dbv* biosynthetic cluster devoted to A40926 production. A recent work indicates that the MIC of *Nonomuraea* sp. ATCC 39727 toward A40926 during vegetative growth was 4 g/ml, but this increased to ca. 20 g/ml during A40926 production (Marcone *et al* 2010). This result indicates that resistance to A40926 is regulated by A40926 production.

RT-PCR analysis shows that the transcript levels of *dbv6* and *dbv22* genes are constant over time (Alduina *et al*., 2007). Therefore it can be assumed that the *dbv6* and *dbv22* genes are constitutively transcribed; in the presence of an inducer molecule (which may be the same antibiotic) Dbv22 could activate Dbv6 by phosphorylation and Dbv6 could activate *vanY* transcription.

Materials and Methods

Bacterial strains, cloning vectors and cultivation

Nonomuraea strains ATCC 39727, Ko *dbv4,* Ko *dbv3* and over *dbv3* were cultured in R3 medium and plated on R3 (Shima, 1996), V0.1 (Marcone, 2010), MS (Kieser, 2000). *Escherichia coli* DH10B (Invitrogen) was used as general cloning host. *E. coli ET12567 [pUZ8002]* was used as donor in intergeneric conjugations (MacNeil, 1992). *E. coli BW25113* (Datsenko, 2000) was used as the host for Red recombination. The integrative vector pIJ8600 was used for gene over-expression. Antibiotic assays were carried out against *Micrococcus luteus* ATCC 9341 (Kovacs, 1999).

All flask cultures were incubated at 30°C on a rotary shaker (200 rpm), using 250-ml baffled flasks. Frozen cell stocks of the parent and the mutant strains were prepared by storing at −80°C individual aliquots of the desired strain from mid-exponential cultures in medium R3. Seed cultures were prepared by inoculating 0,2 ml of the frozen cell stock into 20 ml of fresh R3 medium, which was incubated for 120 hours, before transferring 1 ml into 50 ml of fresh R3 medium. Aliquots at different time points were taken and stored at -80°C.

For HPLC analysis, samples were mixed with 2 volumes of methanol, mixed briefly, followed by 1 h incubation at 40°C. After centrifugation to remove cells, the clear supernatant was used for high performance liquid chromatography (HPLC) analysis.

Genetic procedures

Standard genetic techniques with *E. coli* and in vitro DNA manipulations were as described by Sambrook, Fritsch and Maniatis (1989).

Recombinant DNA techniques in *Streptomyces* species and isolation of *Streptomyces* total DNA were performed as described by Kieser (2000). Southern hybridization was carried

out with probes labeled with digoxigenin by using the DIG DNA labeling kit (Roche Biochemicals). Intergeneric conjugation between *E. coli ET12567* [pUZ8002] and *Nonomuraea* strains was performed as previously described (Stinchi *et al.*, 2003).

Construction of Knock out mutants

Deletion of *dbv3* and *dbv4* from *Nonomuraea* was made by replacing the wild-type gene with a cassette containing an apramycin selective marker using a PCR based system (Kieser 2000). The plasmid pIJ773 containing the apramycin resistance gene (*aac*(3)IV) and the oriT replication origin was used as a template. The knock out mutant in *dbv3* was constructed using the oligonucleotides *dbv3* tar for and *dbv3* tar rev (see table 1). The knock out mutant in *dbv4* was constructed using the oligonucleotides *dbv4* tar for and *dbv4* tar rev.

These long PCR primers were designed to produce a deletion of *dbv4* gene from 39 bp downstream its start codon to 41 bp upstream its stop codon and respectively 98bp and 53bp for *dbv3* gene.

The 39 sequence of each primer matches the right or left end of the disruption cassette (the sequence is shown uppercase in both primers). The extended resistance cassette was amplified by PCR and *E. coli BW25113*/pIJ790 bearing cosmid 11A5 (Sosio *et al*., 2003) was electro-transformed with this cassette. The isolated mutant cosmid was introduced into the non-methylating *E. coli ET12567* containing the pUZ8002. The mutant cosmid was then transferred to *Nonomuraea* ATCC 39727 by intergeneric conjugation. Double cross-over conjugants were screened for their apramycin resistance and analyzed by PCR, using respectively the primers *Ko dbv3 for* and *Ko dbv3 rev* to confirm Ko *dbv3* mutant, and *Ko dbv4 for* and *Ko dbv4 rev* to confirm Ko *dbv4* mutant. The PCR products were sequenced (BMR Genomics).

Construction of over *dbv3* mutant

The integrative vector pIJ8600 was used for *dbv3* gene over-expression. PCR fragment was prepared using the primers over dbv3 for and over dbv3 rev, cloned into pGEM T-Easy vector (Promega), digested with *Bgl*II (Invitrogen) and *Nde*I (Invitrogen). This fragment was cloned into the *Bam*HI (Invitrogen) and *Nde*I site of pIJ8600. The plasmids were transferred to *Nonomuraea* by conjugation from *E. coli ET12567 [pUZ8002]* as described previously. A control strain was prepared by transferring pIJ8600 to *Nonomuraea*.

Nucleic acid extractions

RNA was extracted using the RNeasy® midi Kit after 48 and 72 h of growth. Briefly, four ml from liquid cultures were harvested by centrifugation; and frozen at -80°C. The mycelium was then added to P buffer (Kieser, 2000). in the presence of lysozyme (50mg/ml). RNeasyMini Spin columns were used for RNA isolation according to manufacturer's instructions. RNA preparations were treated twice with DNase I (Roche) in order to eliminate chromosomal DNA contamination. The absence of DNA was confirmed by PCR with recombinat Taq DNA polymerase (Invitrogen). Total RNA concentration was determined with a NanoDrop ND-1000 spectrophotometer (Thermo Scientific), and quality and integrity were checked in an agarose gel.

Gene expression analysis by Reverse Transcriptase PCR

Transcription was studied by using the SuperScriptTM One-Step RT-PCR system with PlatinumH Taq DNA polymerase (Invitrogen), using 100 ng of total RNA as template. Conditions were as follows: first strand cDNA synthesis, 50°C for 30 min followed by 95°C for 10 min; amplification, 30 cycles of [95°C for 30 sec, 66°C for 30 sec, and 72°C for 30 sec]. Primers (18–25 mers,) were designed to generate PCR products of

approximately 200–500 bp. Negative controls were carried out with each set of primers and PlatinumH Taq DNA polymerase in order to confirm the absence of contaminating DNA in the RNA preparations.

qRT-PCR

RNAs were converted in cDNAs using High Capacity cDNA Reverse Transcription Kit (Applied Biosystems) and 100 ng of total RNA as template. Power SYBR® Green (Applied Biosystems) was used for qRT-PCRs, and reactions were run on a Applied biosystem 7300 Real-time PCR System (Applied Biosystems). Reactions were carried out by triplicate and appropriate controls were included to verify the absence of gDNA contamination in RNA, and primer-dimer formation. Primers were designed to generate PCR products between 200 and 350 bp. The PCR reactions were initiated by incubating the sample at 95°C for 10 min followed by 40 cycles at 95°C for 15 s, 64°C for 60 s. The expression of the *Nonomuraea hrdB* gene, likely to encode a constitutive vegetative sigma factor or 16S RNA, were used as an internal control to quantify the relative expression of target genes. To check the specificity of qRT-PCR reactions, a DNA melting curve analysis was performed by holding the sample at 60°C for 60 s followed by slow ramping of the temperature to 98°C. SYBR fluorescence was normalized by ROX fluorescence.

Microbiological assay for A40926 production

A dense suspension of *Micrococcus luteus* was prepared in sterile water at the OD600=1.2.

Transfer 100 µl of bacterial suspension in a falcon with 7ml of soft agar and pour on a plate of LB agar. When the soft agar becomes solid, pieces of 3MM paper containing supernatants of cultures were added.

Feeding experiments

Sources of carbon added to 20 ml of minimal medium:

625 µl of 40% glycerol in order to obtain a final concentration of 1% glycerol;

500 µl of a solution obtained by dissolving 1g of yeast extract, 5 ml of water (0.1 g of yeast extract per 20 ml of minimal medium);

40 µl of 1M citric acid (final concentration);

20 µl of 3M sodium acetate in order to obtain a final concentration of 0.3 10-3M.

S1 mapping high resolution

Probe was generated by PCR: the downstream primer 4_DWnew was phosphorylated using γ^{32}P and T4 polynucleotide kinase; the PCR was performed using the radiolabelled primer and the unlabeled upstream primer. To differentiate probe-probe reanniling and full length protection, the upstream primer was incorporate with a non-homologous tail at the 5' end. Then 40 µg of RNA and 30 fmole probe were mixed together , dry in speed vacuum and resuspended in 20 µl of NaTCA hybridization solution (Summerton, 1983). The tube was placed in a 70°C bath for 10 minutes and transferred at 45°C for 15 hours. 300 µl of chilled 5x S1 digestion buffer (1,4 M NaCl; 150 mM sodium acetate pH4.4; 22,5 mM zinc acetate; 100 µg/ml denatured non homologous DNA) containing 100 units S1 nuclease was added to the tube and then it was placed in ice. The sample was incubated at 37°C for 45 minutes and 75 µl of S1 termination solution (2,5 M ammonium acetate, 0,05M EDTA) were added to the sample. 10 µg of carrier tRNA and 400 µl of isopropanol were added to the sample and after 10 minutes on ice, it was spinned and pellets were resuspended in S1 loading buffer (80% formamide, 10 mM NaOH, 1mM EDTA, 0,1% bromophenol blue). After denaturation (90-100°C for 2 minutes), run was performed on a

conventional 6% polyacrylamide-urea sequencing gel, alongside an appropriate sequencing ladder. The gel was exposed to X-ray film.

Total Protein extraction

The cells after 96 hours of growth in Rare 3 were resuspended in crack buffer (10 mM Tris-HCl [pH 8.0], 0.5 mM EDTA, 0.3 mM DTT) in a volumetric ratio of 1:1 and were then lysed by sonication (using the ultrasonic generator Vibra-cell, Sonic & Material) with four pulses of 30 seconds (% duty cycle: off, output control: 4). The suspension was centrifuged at 12,000 rpm for 15 minutes at 4° C and the spent medium was recovered and stored at -80°C (termed crude extract).

Fractionation by precipitation in ammonium sulfate

The total of $(NH4)_2SO_4$ with which to treat the crude extract was added slowly and the samples were incubated at 4°C for one hour in ice and the centrifuged at 10,000 rpm for 10 min in tubes corex. The pellets were resuspended in 4 ml of water milliQ sterilized and stored at -80 ° C. The procedure was performed three times, namely those required to subdivide the crude extract in three ranges of ammonium solfato : 0-30% , 30-60 % and 60-100%. To determine the amount of ammonium sulphate , needed to reach a certain saturation percentage , was applied to the following formula : $G= \frac{533\ (S_2-S_1)}{100-(0,3\ S_1)}$ where S1 is the saturation percentage of the initial solution , S2 is the percentage of saturation of the final solution, and G is the weight in grams of ammonium sulfate to add to a liter of solution.

To 5 ml of crude extract were added 0.7995 g of (NH4) 2SO4 . The amount of ammonium sulfate added to cover the subsequent saturation was determined in based on the volume of the supernatant, which is subject to change after the first addition the first aliquot of ammonium sulfate. The fractions from the ammonium sulfate precipitation were dialyzed

using the dialysis membranes NeflexTM (Union Carbide©). The samples were inserted into dialysis membranes and dialyzed against distilled water for one hour. The procedure was repeated two more times and then over night.

Preparation of double-stranded oligonucleotides

The preparation of the oligonucleotide double-stranded P4 of 43 bp, biotinylated not, was made from the single-stranded filaments :

FOR: 5'ATCGAATTGCAGAACGCTTCCCGTTAGCATTCCGATCACTCCG3 '

REV: 5'CGGAGTGATCGGAATGCTAACGGGAAGCGTTCTGCAATTCGAT3 '

The oligonucleotides were resuspend in H_20 to obtain a final concentration of 2 g/L. Equal amounts of the two complementary oligonucleotides (25 to 100 g) were mixed in Buffer M Boehringer©, for a final volume of 200 µl. This mix was boiled for 5 minutes, then cool down slowly to 4°C and the probe was purified on a 20% non-denaturing polyacrylamide gel. The gel portion of the gel containing the oligonucleotide double-stranded was taken with a scalpel, placed in a eppendorf tube and DNA was eluited from the gel according to the crush- soak method (Sambrook J. *et al.*, Molecular Cloning : a Laboratory Manual, 1982). The DNA was resuspended in sterilized milliQ H_2O.

The marking of the oligonucleotide double-stranded P4 has provided for the use of T4 polynucleotide kinase (Invitrogen ™) and has complied with the protocol of the supplier.

For purification from excess nucleotides have been used columns MicroSpin™ G-25 Columns (GE Healthcare, Amersham©).

Affinity chromatography

For the affinity chromatography that uses the biotin-streptavidin system and as resin marbles metal MagneSphere® Magnetic Promega© (1 mg/ml) P4 DNA was used at a concentration of 30 ng/L. The protein fractions have been used to concentration of 0.2

mg/ml in Lysis Buffer, together with 1mM PMSF (protease inhibitor) and poly d(I)-d(C) or alternatively in Lysis Buffer and poly d(I)-d(C).

Aliquot 200 µl of MagneSphere Magnetic® were prepared in three 1.5 ml tubes : A, control only MagneSphere®; B, control and extract only MagneSphere® protein; C, samples with MagneSphere®, DNA and protein extract. The three mixes were incubate for 2 minutes in a magnetic rack, the supernatant was removed and MagneSphere® were resuspended in 100 µl of Wash Buffer 2X. This wash was repeated three times. At the end MagneSphere® were resuspended in 200 µl of Wash Buffer 2X. 200 µl of sterilized milliQ H_2O was added in the samples A and B, and 200 µl of DNA in the sample C. the samples were incubated 2 minutes into a thermo mixer at 22°C, mixed manually every 5 minutes to resuspend the MagneSphere®, incubated for 2 minutes in a magnetic rack. The supernatant was removed and MagneSphere® were resuspended in 1 ml of 1X Wash Buffer. This wash was repeated three times. MagneSphere® of sample A were resuspended in 600 µl of Lysis Buffer; samples B and C in 600 µl of protein sample. The samples were incubated 2 hours at 22°C in thermo mixer, shaked manually every 20 minutes to resuspend the best MagneSphere. The samples were incubated for two minutes on a magnetic rack, the supernatant (which contained the unbound protein fraction) was recovered and MagneSphere® were resuspended in 50 µl of Elution Buffer and incubated for 10 minutes at 22°C in a thermomixer. After incubation for 2 minutes in a magnetic rack and the supernatant (eluate) was recovered. At the end of each incubation in thermo mixer is possible to subject the samples to a mild centrifugation at 500-1000 rpm for 10-15 seconds.

Ion exchange chromatography

The ion exchange chromatography uses a FPLC system. Mono Q PC 1.6/5™ (Amersham Pharmacia Biotech) columns of 1 ml were used. The samples were filtered through a filter of 0.22 mM and then loaded into the column. For loading and elution were used two

buffers: 0.05 M Hepes+NaCl, 0.05 M Hepes pH 8 and 0.05 M NaCl+1M pH8. The relationship between the two buffers, which determines the final concentration of the eluent, is finely adjusted through a computerized system that controls the concentration of high-salt buffer and the flow rate (1 ml/min). The liquid exiting from the column reaches a detector (AUSF: 0.02), which will draw a chromatogram. 15 fractions were collected using increasing concentrations of NaCl from 0.25 M to 2M. The protein fractions, because of the high salt concentrations, were dialyzed against Distilled H_2O, before being subjected to other analysis.

EMSA

For electrophoretic mobility shift assays (EMSA) non-denaturing 5% polyacrylamide gel were used. The polymerization took place under the hood chemistry in a chamber formed by electrophoretic glasses 17X16 cm 3 mm thickness and spacers of 1.5 mm.

10 µl of protein sample was thawed slowly on ice, incubated for 20 minutes in ice together with 2 µl of sterilized milliQ H_2O, 2 µl of 50% glycerol, 2 µl of 10X BB (binding buffer), 1 µl of 10 mM MgCl2, 1 µl of poly d(I) - d(C) (Nonspecific DNA). After that, the probe was added (P4 labeled with γ32 -ATP) to concentration of 0.2 ng/L and the mixture was incubated for 15 minutes on ice. The running was conducted at 160 Volts and 20mA. The running buffer is the 0.5X TBE. The gel was removed from the electrophoretic chamber, adsorbed to a sheet of 3 mm paper and dried over Gel-dryer at 80°C for 1 hour. Once dried, the gel was exposed against an autoradiographic film, for the desired time. The autoradiographic film has been developed and fixed in the darkroom thanks to Kodak reagents. Subsequently was made to dry at 37° C for 30 minutes.

Table 4. Primers used in this work

primer name	primer sequence	use
16s nono left 16s nono right	AGCTTGTTGGTGGGGTAGTG TCACCGCTACACCAGGAATT	endogenous control in qRT-PCR
hrdb rev *hrdb* for	CTGGCGGATGCGCTCACGCGTGAC CTCGCTGGCCAAGCGCTACACCGG	endogenous control in qRT-PCR
dbv3 rt rev *dbv3* rt for	GCCGGCTGGACGTGAAGGTGA CGACACTCCGCCCAGCAGCAG	qRT-PCR of *dbv3* gene
dbv4 rt rev *dbv4* rt for	GCTCCAACCGGCCTCTCACATC GGGGTGAAACAACAATCTCGGTGA	qRT-PCR of *dbv4* gene
dbv6 rt for *dbv6* rt for	AGCCTGGGCGCCGACGACTAT GCGCGGGACGGTTTCGATCA	qRT-PCR of *dbv6* gene
dbv14 rt rev *dbv14* rt for	AGCATGTCGTCGCCGGGATC GGTGCTGGGCTCGGACAAGTTC	qRT-PCR of *dbv14* gene
dbv15 rt rev *dbv15* rt for	GATGAGACTCTTCGGCCGGATGT CGGCTCCTTCCTCGTGCTCGT	qRT-PCR of *dbv15* gene
dbv20 rt rev *dbv20* rt for	GCCGCTGATCGAGGAACGCC CGCCCGAATCGTGTCATGAA	qRT-PCR of *dbv20* gene
dbv26 rt rev *dbv26* rt for	CGCCCGAATCGTGTCATGGAA GCCGCTGATCGAGGAACGCC	qRT-PCR of *dbv26* gene
dbv28 rt rev *dbv28* rt for	TCCGCTACTGGGGGCACGC CGGCGGATATGGCGGTAGAGAA	qRT-PCR of *dbv28* gene
dbv29 rt rev *dbv29* rt rev	CCCGCTGTTCCGCTCGTACCA CCTGATCGAGCCGGGCAACAC	qRT-PCR of *dbv29* gene
dbv34 rt for *dbv34* rt for	CGGCCAGGACCTCAAGGAACG GGCCACCGACCGATCCAGCT	qRT-PCR of *dbv34* gene
dbv36 rt rev *dbv36* rt for	CGGGCAGGACGTGGCAGGAG CGGGCACAGTATGGGCAGTTTG	qRT-PCR of *dbv36* gene
dbv37 rt rev *dbv37* rt rev	ACCGCCTCCCCACGCTGAAG CGGGTTGAGCAGGCTGATCGAC	qRT-PCR of *dbv37* gene
left ko2 *iclR* left ko1 *iclR*	GGTGATGAACGGGTCTGC TTCACTGGCTCAGCTCGTC	qRT-PCR of *iclR* gene

primers name	**primers sequence**	**use**
dbv3-apra for	GCCGGCCGCGGTGGAGTGGGCGTCATCAC-GGGGCCTGTGATTCCGGGGATCCGTCGACC	to generete Ko *dbv3* mutant
dbv3 apra rev	CCTCACGCGGCTCGCGGCCGGCTGTGGCCGT-CGCCTTCTTGTAGGCTGGAGCTGCTTC	
dbv4-apra for	GTGGACCCGACGGGAGTTGACATAGCCAC-TCTCCCTGTCATTCCGGGGATCCGTCGACC	to generete Ko *dbv4* mutant
dbv4 apra rev	AGCGGCCAGATCGGTCGCCCGCCCCTCCA-GGCGATCCGCTGTAGGCTGGAGCTGCTTC	
dbv6-apra for	ATGCGCGTTCTGGTGGTGGAGGACCAAGT-CGACCTGGCCATTCCGGGGATCCGTCGACC	to generate Ko *dbv6* mutant
dbv6 apra rev	ATGCGATATCCCTCGCGCGGGACGGTTT-CGTCGCCTTCTTGTAGGCTGGAGCTGCTTC	
dbv22-apra for	GTGGCCCATCGTCTCCGACGCCTGACAA-CAGCCTTCCGCATTCCGGGGATCCGTCGACC	to generate Ko *dbv22* mutant
dbv22 apra rev	GGATGGCGCCAGCCGGCGCAGCGCGCGCC-GCATGAGGGGTGTAGGCTGGAGCTGCTTC	
Ko *iclR* rev	AAGCTTGTGCAGCCGGTCGGGCTCCT	to generate Ko *iclR* mutant
Ko *iclR* for	AAGCTTCAATGCCCTGGAAGCGGGAC	
dbv3 tar *rev*	TCACAGCAGATTCCGGTACA	to distinguish Ko *dbv3* mutant from wild type
dbv3 tar *for*	GATGAGCACGAGTGGATGAG	
dbv4 tar for	ACTTGGCCGATCGATTTATG	to distinguish Ko *dbv4* mutant from wild type
dbv4 tar rev	GAATCGAGCAACCTCGTCAG	
dbv6 tar for	ACGCGAGCTATGGTGTCAG	to distinguish Ko *dbv6* mutant from wild type
dbv6 tar rev	GCTTCTCCTCATCCCTCTCC	
dbv22 tar for	GTGCGCTGACTCGGTAGG	to distinguish Ko *dbv22* mutant from wild type
dbv22 tar rev	ACGTTCTCTGACCAGCCTGT	
f_*dbv3* (NdeI):	AAAAAAAACATATGCTGTTCG GGCGAGATCG	to generate the over *dbv3* mutant
r_*dbv3* (BglII):	AAAAAGATCTCTACAGCCGCACTGCCTCAC	
f_*iclR*(NdeI)	AAAAAAAACATATGTCGAGACTGCAGTATCG	to generate the over *iclR* mutant
r_*iclR*(BamHI)	AAAGGATCCTCATGACGTGCGGCGCATCG	
iclR-BamHI	GGATCCAATGTCGAGACTGCAGTATCG	to overexpress 6 his tagged IclR in *E. coli*
iclR-HindIII	AAGCTTTCATGACGTGCGGCGCATCG	
pIJ8600 r	TCACTCCGCTGAAACTGTTGA	to amplified insert in pIJ8600
pIJ8600 l	GGTTGGACAGGGCTGAGG	

References

Alduina R., Lo Piccolo L., D'Alia D., Ferraro C., Gunnarsson N., Donadio S., and Puglia A. M., (2007). **Phosphate-Controlled Regulator for the Biosynthesis of the Dalbavancin Precursor A40926**. J. of Bacteriology, p. 8120–8129 Vol. 189, No. 22.

Binda E., Marcone G. L., Pollegioni L. and Marinelli F., **Characterization of VanYn, a novel D,D-peptidase/ D,D-carboxypeptidase involved in glycopeptide antibiotic resistance in *Nonomuraea* sp. ATCC 39727** FEBS Journal 279 (2012) 3203–3213

Chen A. Y., M. J. Zervos, J. A. Vazquez, (2007), **Dalbavancin: a novel antimicrobial**. J Clin Pract, May 61, 5, 853–863.

Chen J. and Jianping Xie, (2011), **Role and Regulation of Bacterial LuxR-Like Regulators**, J. Cell. Biochem. 112: 2694–2702, 2011.

Cozzone A. J., Mansi El-Mansi, (2005) **Control of Isocitrate Dehydrogenase Catalytic Activity by Protein Phosphorylation in *Escherichia coli*.** J Mol Microbiol Biotechnol 9:132–146.

Dalebroux Z. D. and Swanson M. S. **ppGpp: magic beyond RNA polymerase** Nature Reviews **Microbiology** Volume 10, March 2012 ;10(3):203-12.

Deghorain M., Goffin P., Fontaine L., Mainardi J.-L., Daniel R., Errington J., Hallet B., and Hols P., (2007), **Selectivity for D-Lactate Incorporation into the Peptidoglycan Precursors of *Lactobacillus plantarum*: Role of Aad, a VanX-Like D-Alanyl-D-Alanine Dipeptidase**. J. Of Bacteriology, June 2007, p. 4332–4337 Vol. 189, No. 11.

Dorr M. B., Jabes D., Cavaleri M., Dowell J., Mosconi G., Malabarba A., White R. J. and Henkel T. J., (2005) **Human pharmacokinetics and rationale for once-weekly dosing of dalbavancin, a semi-synthetic glycopeptide**. J. of Antimicrobial Chemotherapy 55, ii25–ii30. pag. 68

Eusta´quio A. S., Li S.-M. and Heide L. **NovG, a DNA-binding protein acting as a positive regulator of novobiocin biosynthesis.** Microbiology (2005), 151, 1949–1961

Fuqua W.C., Winans S. C., and Greenberg E. P. **Quorum Sensing in Bacteria: the LuxR-LuxI Family of Cell Density-Responsive Transcriptional Regulators.** J. Of Bacteriology, Jan. 1994, p. 269-275 Vol. 176, No. 2

Ghorbel S., Smirnov A., Chouayekh H., Sperandio B., Esnault C., Kormanec J., and Virolle M.-J. (2006) **Regulation of ppk Expression and In Vivo Function of Ppk in *Streptomyces lividans* TK24.** J. Of Bacteriology, Sept. 2006, p. 6269–6276 Vol. 188, No. 17.

Goldstein B. P., Selva E., Gastaldo L., Berti M., Pallanza R., Ripamonti F., Ferrari P., Denaro M., Arioli V., e Cassani G. (1987), **A40926, a New Glycopeptide Antibiotic with Anti-Neisseria Activity**. Antimicrobial Agents and Chemotherapy, p. 1961-1966 Vol. 31, No. 12.

Goranovič D., Blažič D., Magdevska V., Horvat J., Kuščer E., Polak T., Santos-Aberturas J., Martínez-Castro M., Barreiro C., Mrak P., Kopitar G., Kosec G., Fujs Š., Martín J. F. and Petković H. **FK506 biosynthesis is regulated by two positive regulatory elements in *Streptomyces tsukubaensis***. BMC Microbiology 2012, 12:238

Guerra S. M., Rodrıguez-Garcıa A., Santos-Aberturas J., Vicente C. M., Payero T. D., Martın J. F., Aparicio J. F. (2012), **LAL Regulators SCO0877 and SCO7173 as Pleiotropic Modulators of Phosphate Starvation Response and Actinorhodin Biosynthesis in *Streptomyces coelicolor*.** *PLoS ONE*, Volume 7, Issue 2.

Gunnarsson N., Bruheim P., Nielsen J., (2003) **Production of the glycopeptide antibiotic A40926 by *Nonomuraea sp. ATCC 39727*: influence of medium composition in batch fermentation** , J. Ind. Microbiol. Biothecn. (2003) 30: 150–156.

Gunnarsson N., Bruheim P., Nielsen J. **Glucose Metabolism in the Antibiotic Producing Actinomycete *Nonomuraea* sp. ATCC 39727** 7 Biotechnol Bioeng. 2004 Dec 5;88(5):652-63.

Gunnarsson N., Mortensen U. H., Sosio M. and Nielsen J**. Identification of the Entner–Doudoroff pathway in an antibiotic-producing actinomycete species** Molecular Microbiology (2004) (3), 895–902

Guo D., Zhao Y., Yang K., **Coordination of glycerol utilization and clavulanic acid biosynthesis to improve clavulanic acid production in *Streptomyces clavuligerus*** Biotecnologie Microbiche Casa Editrice Ambrosiana. SPECIAL TOPIC: Biosynthesis and regulation of secondary metabolites in microorganisms July 2013 Vol.56 No.7: 591–600

He W., Lei J., Liu Y., Wang Y. **The LuxR family members GdmRI and GdmRII are positive regulators of geldanamycin biosynthesis in *Streptomyces hygroscopicus* 17997** Arch Microbiol (2008) 189:501–510

He X., Li R., Pan Y., Liu G., and Tan H. **SanG, a transcriptional activator, controls nikkomycin biosynthesis through binding to the *sanN–sanO* intergenic region in *Streptomyces ansochromogenes*.** Microbiology (2010), 156, 828–837

Horinouchi S., **A microbial hormone, A-factor, as a master switch for morphological differentiation and secondary metabolism in *Streptomyces griseus***, Frontiers in Bioscience 7, d2045-2057, October 1, 2002

Hubbard B. K., Thomas M. G., Walsh C.T. **Biosynthesis of L-p hydroxyphenylglycine, a non-proteinogenic amino acid constituent of peptide antibiotics.** Chemistry & Biology, (2000), volume 7, p. 931-942.

Hutchings M. I., Hong H.-J. and Buttner M. J. **The vancomycin resistance VanRS two-component signal transduction system of *Streptomyces coelicolor*** Molecular Microbiology (2006) **59** (3), 923–935

Jovetic S. , Zhu Y., Marcone G. L., Marinelli F., Tramper J. (2010), **β-Lactam and glycopeptide antibiotics: first and last line of defense?** Trends in Biotechnology, Volume 28, Issue 12, December 2010, 596–604.

Kieser T., Bibb M. J., Buttner M. J., Chater K. F., Hopwood D. A.. (2000) **Practical *Streptomyces* Genetics.**

Kruger R. G. , Lu W., Oberthür M., Tao J., Kahne D., Walsh C. T., (2005), **Tailoring of Glycopeptide Scaffolds by the Acyltransferases from the Teicoplanin and A-40,926 Biosynthetic Operons**, Chemistry & Biology Volume 12 pag 131-140. pg. 69

Kusˇcˇer E., Coates N., Challis I., Gregory M., Wilkinson B., Sheridan R., and Petkovic´ H. **Roles of *rapH* and *rapG* in Positive Regulation of Rapamycin Biosynthesis in *Streptomyces hygroscopicus*.** J. Of Bacteriology, July 2007, p. 4756–4763 Vol. 189, No. 13

Leipe D. D., Koonin E. V. and Aravind L. **STAND, a Class of P-Loop NTPases Including Animal and Plant Regulators of Programmed Cell Death: Multiple, Complex Domain Architectures, Unusual Phyletic Patterns, and Evolution by Horizontal Gene Transfer** J. Mol. Biol. (2004) 343, 1–28

Malabarba A. and Goldstein B. P., (2005) **Origin, structure, and activity in vitro and in vivo of dalbavancin**. *J*. of Antimicrobial Chemotherapy 55, Suppl. S2, ii15–ii20.

Manteca A., Sanchez J., Jung H. R., Schwammle V., Jensen O. N.,(2010), **Quantitative Proteomics Analysis of *Streptomyces coelicolor* Development Demonstrates That Onset of Secondary Metabolism Coincides with Hypha Differentiation.** Molecular & Cellular Proteomics 9:1423–1436.

Marcone G. L., Beltrametti F., Binda E., Carrano L., Foulston L., Hesketh A., Bibb M., and Marinelli F.,(2010), **Novel Mechanism of Glycopeptide Resistance in the A40926 Producer *Nonomuraea* sp. ATCC 39727**. Antimicrobial Agents And Chemotherapy, p. 2465–2472 Vol. 54, No. 6.

Marcone G. L., Foulston L., Binda E., Marinelli F., Bibb M., Beltrametti F. **Methods for the genetic manipulation of *Nonomuraea* sp.ATCC 39727** J Ind Microbiol Biotechnol (2010) 37:1097–1103

Martín J. F. (2004), **Phosphate Control of the Biosynthesis of Antibiotics and Other Secondary Metabolites Is Mediated by the PhoR-PhoP System: an Unfinished Story.** J. Of Bacteriology, Aug. 2004, p. 5197–5201 Vol. 186, No. 16.

Miller M. B. and Bassler B. L. **Quorum sensing in bacteria** Annu. Rev. Microbiol. 2001. 55:165–99

Molina-Henares A. J., Tino Krell, Guazzaroni M. E., Segura A. e Ramos J. L., (2006) **Members of the IclR familyof bacterial transcriptional regulators functionas activators and/or repressors**. *FEMS Microbiol Rev* 30 157–186.

Monciardini P. e Sosio M. (2004), **Reclassification as a *Nonomuraea* sp. of the strain ATCC 39727, producing the glycopeptide antibiotic A40926**, J. Of Antibiotics, Volume 57(1) pag. 68-70.

Ohnishi Y., Yamazaki H., Kato J., Tomono A., Horinouchi S. **AdpA, a central transcriptional regulator in the A-factor regulatory cascade that leads to morphological development and secondary metabolism in *Streptomyces griseus*.** Biosci. Biotechnol. Biochem., 69 (3), 431-439, 2005

Paloma L. J.-F. M. (2010), **Engineering of regulatory cascades and networks controlling antibiotic biosynthesis in *Streptomyces***, Current Opinion In Microbiology, Volume 13, Issue 3, Pages 263–273.

Pfeifer V., Graeme J. N., Recktenwald J. R. J., Schefer A. B., Shawky R. M., Schroder J., Wohlleben W.**,** and Pelzer S.**,**(2001), **A polyketide synthase in glycopeptide biosynthesis the biosynthesis of the non-proteinogenic amino acid (s)-3,5-dihydroxyphenylglycine.** J. Of Biological Chemistry Vol. 276, No. 42, Issue of October 19, pp. 38370–38377.

Pompeani A. J., Irgon J. J., Berger M. F., Bulyk M. L., Wingreen N. S. and Bassler B. L., (2008) **The Vibrio harveyi master quorum-sensing regulator, LuxR, aTetR-type protein is both an activator and a repressor: DNA recognition and binding specificity at target promoters.** Molecular Microbiology 70(1), 76–88.

Qin N., Callahan S. M., Dunlap P. V., and Stevens A. M., (2007), **Analysis of LuxR Regulon Gene Expression during Quorum Sensing in *Vibrio fischeri*,** J. Of Bacteriology, p. 4127–4134, Vol. 189, No. 11. pag. 70

Sakoulas G, Moellering RC Jr, (2008) ,**Increasing antibiotic resistance among methicillin-resistant *Staphylococcus aureus* strains,** Clin. Infeect. Did., Suppl 5:S360-7.

Salehghamari E., Hamedi J., Elahi E., Sepehrizadeh Z., Sadeghi M., Muthn G., (2012), **Prediction of the *pho* regulon in *Streptomyces clavuligerus* DSM 738**. New Microbiologica, 35, 447-457.

Sambrook, J., Fritsh, E. F., Maniatis, T. (1989).**Molecular cloning. A laboratory manual.**

Santamarta I., López-García M. T., Pérez-Redondo R., Koekman B., Martín J. F. e Liras P., (2007) **Connecting primary and secondary metabolism: AreB, an IclR-like protein, binds the ARE *ccaR* sequence of *S. clavuligerus* and modulates leucine biosynthesis and cephamycin C and clavulanic acid production**. Molecular Microbiology 66(2), 511–524.

Santos-Beneit F., Rodríguez-García A., and Martín J. F.,(2011), **Complex Transcriptional Control of the Antibiotic Regulator afsS in *Streptomyces*: PhoP and AfsR Are Overlapping, Competitive Activators,** J. Of Bacteriology, p. 2242–2251 Vol. 193, No. 9.

Sekurova O. N., Brautaset T., Sletta H., Borgos S. E. F., Jakobsen Ø. M., Ellingsen T. E., Strøm A. R., Valla S., and Zotchev S. B. **In Vivo Analysis of the Regulatory Genes in the Nystatin Biosynthetic Gene Cluster of *Streptomyces noursei* ATCC 11455 Reveals Their Differential Control Over Antibiotic Biosynthesis**. J. Of Bacteriology, Mar. 2004, p. 1345–1354 Vol. 186, No. 5

.

Septer A. N., Stabb E. V., (2012) **Coordination of the Arc Regulatory System and Pheromone-Mediated Positive Feedback in Controlling the *Vibrio fischeri* lux Operon**. Volume 7 Issue 11.

Siculella L., Damiano F., Di Summa R., Tredici S. M., Alduina R., Gnoni G. V. and Alifano P. **Guanosine 5'-diphosphate 3'-diphosphate (ppGpp) as a negative modulator**

of polynucleotide phosphorylase activity in a 'rare' actinomycetes. Molecular Microbiology (2010) 77(3), 716–729

Sosio M., Stinchi S., Beltrametti F., Lazzarini A., and Donadio S. (2003) **The Gene Cluster for the Biosynthesis of the Glycopeptide Antibiotic A40926 by *Nonomuraea* Species** .Chemistry & Biology, Vol. 10, 541–549, June, 2003.

Sosio M. and Donadio S. **Understanding and manipulating glycopeptide pathways: the example of the dalbavancin precursor A40926** (2006) J Ind Microbiol Biotechnol 33: 569–576

Sosio M., Canavesi A., Stinchi S., Donadio S. (2010) **Improved production of A40926 by *Nonomuraea* sp. through deletion of a pathway-specific acetyltransferase.** Appl Microbiol Biotechnol 87:1633–1638

Sosio M., Stinchi S., Beltrametti F., Lazzarini A., and Donadio S. **The Gene Cluster for the Biosynthesis of the Glycopeptide Antibiotic A40926 by *Nonomuraea* Species** (2003) Chemistry & Biology, Vol. 10, 541–549, June, 2003, Elsevier Science Ltd. All rights reserved.

Steiert M, Schmitz FJ, (2002) **Dalbavancin (Biosearch Italia/Versicor).** Curr Opin Investig Drugs. Feb;3(2):229-33.

Stinchi S., Carrano L., Lazzarini A., Feroggio M., Grigoletto A., Sosio M. & Donadio S. **Aderivative of the glycopeptideA40926 produced by inactivation ofthe b-hydroxylase gene in *Nonomuraea* sp. ATCC39727** FEMS Microbiol Lett 256 (2006) 229–235

Tala A., Wang G., Zemanova M., Okamoto S., Ochi K., and Alifano P., (2009). **Activation of Dormant Bacterial Genes by *Nonomuraea* sp. Strain ATCC 39727 Mutant-Type RNA Polymerase.** J. of Bacteriology, p. 805–814. Vol. 191, No. 3.

Traag B. A., Kelemen G. H. and van Wezel G. P., (2004) **Transcription of the sporulation gene *ssgA* is activated by the IclR-type regulator SsgR in a *whi* – independent manner in *Streptomyces coelicolor* A3.** Molecular Microbiology, 985–1000.

Vigliotta G., Tredici S. M., Damiano F., Montinaro M. R., Pulimeno R., Di Summa R., Massardo D. R., Gnoni G. V.,and Alifano P. **Natural merodiploidy involving duplicated *rpoB* alleles affects secondary metabolism in a producer actinomycete.** Molecular Microbiology (2005) 55 (2), 396–412

Wilson D. J., Xue Y., Reynolds K. A., and Sherman D. H **Characterization and Analysis of the PikD Regulatory Factor in the Pikromycin Biosynthetic Pathway of *Streptomyces venezuelae*** J. of Bacteriology, June 2001, p. 3468–3475 Vol. 183, No. 11

Wohlleben W., Mast Y., Muth G., Röttgen M., Stegmann E., Weber T., (2012). **Synthetic Biology of secondary metabolite biosynthesis in actinomycetes: Engineering precursor supply as a way to optimize antibiotic production.** *FEBS Letters* 586 (2012) 2171–2176. pag. 71

Xu G., Wang J., Wang L., Tian X., Yang H., Fan K., Yang K., and Tan H. **"Pseudo"-Butyrolactone Receptors Respond to Antibiotic Signals to Coordinate Antibiotic Biosynthesis**, The Journal Of Biological Chemistry Vol. 285, NO. 35, pp. 27440–27448, August 27, 2010

Yamamoto K. and Ishihama A. (2003) **Two different modes of transcription repression of the *Escherichia coli* acetate operon by IclR**. Molecular Microbiology 47: 183–194.

Yang H., An Y., Wang L., Zhang S., Zhang Y., Tian Y., Liu G. and Tan H. **Autoregulation of *hpdR* and its effect on CDA biosynthesis in *Streptomyces coelicolor.*** Microbiology (2010), 156, 2641–2648

Yang Y. H., Eunjung S., Eun-Jung K., Kwangwon L., Woo-Seong K., Sung-Soo P., Ji-Sook H., Byung-Gee K., (2009) **NdgR, an IclR-like regulator involved in amino-acid-dependent growth, quorum sensing, and antibiotic production in *Streptomyces coelicolor***, Appl. Microbiol. Biotechnol., 82:501–511.

Zahaed E.-M., Gonzalez-Ceron G., and Servın-Gonzalez L., (2006), **A Conserved Inverted Repeat, the LipR Box, Mediates Transcriptional Activation of the**

Streptomyces exfoliatus Lipase Gene by LipR, a Member of the STAND Class of P-Loop Nucleoside Triphosphatases. J. of Bacteriology, p. 7082–7089, Vol. 188, No. 20.

Zheng J.-T., Wang S.-L. and Yang K.-Q. **Engineering a regulatory region of jadomycin gene cluster to improve jadomycin B production in *Streptomyces venezuelae*.** Appl. Microbiol. Biotechnol. (2007) 76:883–888

Zhou Y., Huang H., Zhou P., Xie J., (2012), **Molecular mechanisms underlying the function diversity of transcriptional factor IclR family**. Cellular Signalling 24; 1270-1275.